NOLTR 67-87

PRESSURE-PULSE CHARACTERISTICS OF DEEP EXPLOSIONS AS FUNCTIONS OF DEPTH AND RANGE

21 SEPTEMBER 1967

NOL

UNITED STATES NAVAL ORDNANCE LABORATORY, WHITE OAK, MARYLAND

NOLTR 67-87

47

NOLTR 67-87

PRESSURE-PULSE CHARACTERISTICS OF DEEP EXPLOSIONS AS FUNCTIONS OF DEPTH AND RANGE

by
John P. Slifko

ABSTRACT: Thirty-eight TNT and 18 HBX-3 charges weighing one, eight, and fifty pounds were fired at depths between 500 and 14,000 ft; pressure-time data were measured directly above at 185-ft depth. The shock wave peak pressure was independent of depth and decayed with reduced range as in the shallow water case. Durations were a function of depth alone. Empirical equations were derived which show that all other pressure-pulse characteristics can be expressed as functions of depth as well as range. Values obtained for HBX-3 here gave the same ratios to TNT values as previously found in shallow water.

UNDERWATER EXPLOSIONS DIVISION
EXPLOSIONS RESEARCH DEPARTMENT
U. S. NAVAL ORDNANCE LABORATORY
WHITE OAK, SILVER SPRING, MARYLAND

NOLTR 67-87 21 September 1967

PRESSURE-PULSE CHARACTERISTICS OF DEEP EXPLOSIONS AS FUNCTIONS OF DEPTH AND RANGE

The work reported here was undertaken to provide fundamental data needed in studies of the long-range propagation of explosion pressure pulses in the ocean. This report presents for the first time a method of separating the effects of depth and of range on pressure pulse characteristics. This significant step can best be grasped by looking at Table III (page 36). From this table, pulse characteristics of TNT and HBX-3 explosions can be calculated as functions of range and depth separately or together.

The project was supported by the Advanced Research Projects Agency, under ARPA Order 610, Amendment No. 1, NOL Task No. NOL-785/ARPA. Mention of commercially available products in this report does not constitute criticism or endorsement by the Laboratory.

E. F. SCHREITER

C. J. ARONSON
By direction

CONTENTS

ILLUSTRATIONS

CONTENTS (continued)

TABLES

PRESSURE-PULSE CHARACTERISTICS OF DEEP EXPLOSIONS AS FUNCTIONS OF DEPTH AND RANGE

1. INTRODUCTION

The pressure pulse characteristics for explosive compositions fired at shallow depths have been determined from many underwater explosion tests. References 1-3* describe typical experiments of this sort.

It is far more difficult to find the pressure pulse characteristics of deep explosions. If measurements are made near the surface, long range transmission effects (including refraction) will distort the pressure pulse and the effect of the ambient pressure at the explosion cannot be uniquely determined. If measurements are to be made near the charge, some difficult engineering problems will have to be solved.

One experiment has been carried out to find the effect of depth by simulating the deep ocean pressures in a pressure tank (reference 4). However, the experimental conditions were severely restricted.

Some relatively simple tests have been performed (references 5-7) in which the pressures were recorded just below the water surface and directly above deep explosions. In this case, no distortion of the pressure pulse resulted from refraction, since the propagation of the pressure pulses was essentially normal to the isovelocity layers. However, available data were not examined to determine whether the depth effect on the pressure pulses could be separated from the effects of long range transmission (reference 8).

In the tests reported here, measurements were made just below the water surface directly above deep explosions as in the tests of references 5-7. However, additional shallower shots were included and larger charge weights were fired. This resulted in extending the range of the variables by at least an order of magnitude, thus enabling a better statistical determination of the effect of depth and range.

The effect of depth was determined by assuming the pressure pulse characteristics were proportional to the product of a simple power function of depth and of a power function of reduced range required by the principles of similitude for shallow explosions.

2. EXPERIMENTAL ARRANGEMENTS

The tests were conducted from the USNS GILLIS (AGOR-4) in February and March of 1965 in the Atlantic Ocean approximately 110 to 220 miles east of Eleuthera Island in 2600 to 3000 fathoms of water. These tests were designed by E. A. Christian and were executed under the direction of W. H. Faux, both of this Laboratory.

*References are listed on page 14.

2.1 CHARGES

TNT charges weighing one, eight, and fifty-seven pounds each were fired at several depths between 500 ft and 14,000 ft. The number of each of the charge weights fired at the various depths is given in Table I. The 1-lb and 8-lb charges were cast by NOL into cylinders and with a L/D ratio of about 1.0. These charges were boostered at the top end of the cylinder with 0.0662-lb and 0.221-lb cast pentolite boosters for the 1-lb and 8-lb charges, respectively. The cylindrical boosters were co-axial with the TNT charges, and the top of each booster was flush with the top of the main charge. The other TNT charges fired were 56-lb Mark 2 Mod 3 demolition charges with an additional 1-lb pentolite booster strapped to the top of the container to insure proper detonation; only 7 out of 12 of these detonated. Attempts to fire 1000-lb TNT charges (eighteen Mk 2 Mod 3 charges strapped together with one 56-lb charge boostered as above) were unsuccessful.

One, eight, and fifty-lb HBX-3 charges were fabricated at NOL and were boostered with 0.0662, 0.221, and 1.0 lb of cast pentolite, respectively. These charges and boosters were cylindrical and the boostering geometry was similar to that for the 1- and 8-lb TNT charges. The charge weights and nominal firing depths are also given in Table I.

Eighty lbs of Nitramex explosive was loaded by the manufacturer* into 8-in diameter by 24-in long canisters, and each charge was boostered with a 4-1/2-in diameter by 9-in long primer charge of EL-637 Comp B explosive which was taped to the side of the Nitramex charge. In addition, a 1-lb pentolite booster, with a pressure detonator attached, was taped flush with the primer charge so that it was as nearly as possible in contact with the main charge. The firing depths are given in Table I.

Three cylindrical 1-lb pentolite charges cast at NOL were fired at the depths shown in Table I.

In addition to the 67 charges fired, the following 11 charges failed to detonate properly: 1-lb TNT (1), 8-lb TNT (2), 57-lb TNT (5), 1000-lb TNT (2), and 80-lb Nitramex (1). The 57-lb TNT charges were subsequently investigated. It was found that there were substantial cavities at the top end of the charges (reference 9).

2.2 INITIATING DEVICE AND RIGGING

All charges were initiated with a hydrostatic firing device manufactured by Weston Instruments, Inc., Daystrom Drawing #800AA1000. These devices were designed to initiate special percussion detonators** at nominal depths indicated in Table I. Each detonator contained about 1-1/2 grams of explosive and was mounted in the detonator well of the pentolite boosters. The nominal depths of the firing devices were not sufficiently accurate for our purpose and sonic ranging was used to find more precise depths.

Two methods were used to place charges at the firing depth: Free-fall, in which the armed charge was thrown in the water and sank until the firing device was actuated by the ambient pressure, and wire-guided (reference 6) in which the armed

---

* Nitramex was purchased from the E. I. dePont de Nemours; the composition was 16% TNT, 4% DNT, 30% $NaNO_3$, 35% NH_4NO_3 plus iron and phosphorus.

** Fabricated by the Explosion Dynamics Division of NOL.

TABLE I

NUMBER OF CHARGES FIRED UNDER VARIOUS CONDITIONS

Nominal Depth (ft)	TNT			HBX-3			Nitramex		Pentolite
	1-lb	8-lb	57-lb	1-lb	8-lb	50-lb	80-lb	560-lb	1-lb
500	3	2	--	--	--	--	--	--	1
800	2	2	--	--	--	--	--	--	1
1,200	2	2	--	1	2	--	--	--	--
2,000	2	3	2	1	--	1	--	--	--
3,000	2	1	--	--	--	1	3	--	--
4,500	2	3	2	2	1	1	1	--	--
7,000	3	--	2	--	1	1	1	--	1
10,000	--	--	--	1	1	1	1	1	--
14,000	1	2	1	1	1	1	--	--	--

charge slid down a wire rope held vertical by a 900-lb weight at the deep end. The charge was secured to a light steel frame, the top and bottom ends of which were provided with guides for sliding down the wire rope. The charge was separated from the wire rope by a distance greater than the expected bubble radius; i.e., 2 to 7 ft. This charge was initiated in the same manner as the free-falling charge. Approximately 32% of the attempted firings were wire guided. This technique reduced the relative horizontal displacement of the charge and ship.

2.3 INSTRUMENTATION

The pressure-time data was recorded simultaneously by an Ampex FR-600 on magnetic tape and by oscilloscopes on photographic paper. Both recording methods had the desired capability of providing a permanent record only a minute or two after the events. The tape data was also used in ranging the charge and hydrophone depths.

2.3.1 Sonic Ranging of Charge Depth. The explosion depths were determined from the measurements of the time difference between the arrivals of the surface-bottom and the bottom reflected pressure waves, and from the average velocity-depth profile. The latter was obtained from the velocities calculated from the 900-ft B-T measurements, from the single hydrographic cast made to only 850 meters (2800 ft) supplemented by the results of deep hydrographic casts previously obtained at approximately the same area and time of the year. The B-T measurements were made quite frequently--a total of 52 for the 79 attempted shots--to account for the diurnal temperature changes in the surface layer; the measurements nearest the time of each shot were used.

The sonic signals for ranging the charge depth were picked up by an LC-32* hydrophone which was mounted on 400 ft of low noise coaxial cable and was maintained at a depth of about 190 ft. The output signal of this hydrophone was also used to provide a trip pulse to the oscilloscopes. The hydrophone signal was clipped and amplified** before it was applied to the inputs of channels 10 and 11 of the Ampex FR-600 tape recorder. A time base consisting of 10 kHz signal accentuated every 1, 10, and 100 msec was applied to channel 14. See Figure 1.

2.3.2 Pressure-Time Measurements. The shock wave and bubble pulse pressure-time data were obtained with another LC-32 hydrophone located 5 ft above the hydrophone just described. The hydrophone was mounted on similar low-noise cable; however, it was terminated in a simple RC network (reference 10) to reduce reflections in the cable. The output of the termination network was coupled directly to the input (2.10^7 ohms) of a "K" amplifier (reference 11), the output impedance of which was 100 ohms. A 100 μF condenser was used to couple the output of the "K" amplifier to the inputs of a dual-beam oscilloscope (Tektronix RM 565) and a four-beam Electronic Tube Corporation Model K-47C oscilloscope (Figure 1). In addition, a 200 ohm output of the dual beam scope was coupled with a 40 μF condenser to the input of channel 8 of the FR-600. Thus, it was possible to record from the same hydrophone a total of 10 channels of data, each with different amplification. The 3 dB points of the frequency band were about 0.4 Hz and 20 kHz for the tape data (FM recording at 60 IPS) and about 0.4 Hz and 50 kHz (hydrophone limited) for the oscilloscope data. The data from both oscilloscopes was recorded on photographic paper with Polaroid cameras.

3. ANALYSIS OF DATA

Most of the data analyzed was obtained from channel 8 of the FR-600 tape recorder; the dual beam oscilloscope data was from five shots which were not recorded on the FR-600. In addition, the oscilloscope data from five other shots was analyzed to compare with the FR-600 recordings of the same shots. The programs used on the IBM 7090 computer were essentially the same for the two cases, except that the method of reading the data from the records and the form of the input data differed.

3.1 ANALYSIS OF FM TAPE DATA

The magnetic tape data was digitized by the Mathematics Department of the Naval Ship Research and Development Center on their Computer Data Format Translater (CDFT) which provided a maximum sampling rate of 2000 samples per second. The tape data was first played back on the NSRDC Ampex FR-600 at a speed of 3-3/4*** in/sec, and

---

* Manufactured by Atlantic Research Corp., Alexandria, Va. It should be noted that low frequency distortion was probably introduced by the LC-32 hydrophone. In special shock wave response tests (reference 12) of tourmaline and ceramic gauges at the 100 psi level, it was shown that the pressures from LC-10 and LC-32 gauges decayed too slowly due to a relaxation effect, resulting in large shock wave impulse values. However, it was not determined whether or not the relaxation effect persisted at lower pressure levels, such as those recorded from the deep shots reported here.

** Radiation Electronics Co., Model TA-5 Amplifier.

*** An attempt was made to play back the tapes at 1-7/8 in/sec in order to realize the full band width capabilities of the recorder; i.e., 20 kHz. Unfortunately, this speed resulted in a considerable increase in playback noise level, so the 3-3/4 in/sec speed was used.

the analog output was then sampled and digitized 1875 times/sec on the CDFT. Since the tape data was recorded at 60 in/sec, the sampling rate was equivalent to 30,000 samples/sec in recorded time.

The CDFT digitized tape data was on a low density binary tape containing 21 words per record in which the first word represented the identification number and the time (in msec) of the first sample of that record. The remaining 20 words represented 60 consecutive samples of the pressure or calibration data. The number of records was determined before hand on the basis of the duration of the pulse required to be digitized. Next, a decimal dump of the CDFT digital tape was obtained at NOL by means of the program TESTP (reference 13). The program NEWGRL (reference 13) was then used on the IBM 7090 computer to calculate the maximum pressure, impulse, energy, pulse duration, spectral amplitude and energy density, and the octave band spectral energy of the pressure pulse. The program is quite flexible so that, for instance, the above pulse characteristics can be calculated for any portion of the pressure pulse, the frequency interval in the spectral energy density calculations could be varied, the number of octave bands changed, etc. The program SPRING (reference 13) was used with NEWGRL to provide plots of the amplitude and energy spectra, in dB, as a function of log frequency. Spectral energy data are reported in reference 14.

3.2 ANALYSIS OF OSCILLOSCOPE DATA

The few examples of pressure-time data obtained from oscilloscope records were read manually from photographic films at discrete time increments of equal value (16-2/3 μsec) on the NOL Telereadex. (Photographic films were made from the original Polaroid prints to facilitate the reading of the data on the Telereadex.) Each pressure datum point was punched on an IBM card, and these cards were used with program PAPPY (reference 13) on the IBM 7090 to compute the pulse and spectral characteristics mentioned above.

3.3 ANALYSIS OF ANALOG TAPE DATA

The analog tape data were played back on the NOL FR-600 and a Visicorder* was used to provide a graphical record of pressure as a function of time. All pressure and all time duration values of the various phases of the pressure pulse reported herein were obtained from these records. Only the impulse and energy values reported herein were obtained from the digital tape data; i.e., program NEWGRL. The reason the pressures and time durations were not obtained from the digital data was that the sampling rate was too coarse in many cases to provide accurate peak pressure values and also that the noise on the pressure-time records made it difficult to determine (from program TESTP) the times at which pressures were equal to the ambient pressure. It should be noted, however, that although the maximum pressures may differ by as much as ± 10% by the two methods on some shots, the resulting equations of p_m vs $W^{1/3}/R$ were essentially identical.

4. RESULTS

The shock wave and bubble pulse data are shown in Table II for TNT, HBX-3, pentolite and Nitramex. Representative pressure-time records are reproduced in

* The Visicorder (Model 906B) is a paper recorder complete with 12 channels of amplifiers and a multispeed paper drive. It is manufactured by Honeywell, Inc., Denver, Colorado.

Figures 2 and 3. The TNT and HBX-3 reduced data are plotted in Figures 4 through 16, and the equations of the curves in these figures are summarized in Table III. The sparse data obtained for pentolite and Nitramex were not sufficient for making plots.

In this report, the shock wave is also called "the first positive phase" since all integrations of impulse and energy were carried out to the time at which the shock wave pressures decayed to the ambient pressure level. This crossing point is clearly defined, in contrast to the shock waves from shallow water explosions for which the time at which the pressure decays to ambient pressure is quite uncertain. In all these pressure-time records, the base line; i.e., ambient pressure level, was not adjusted as was done in references 15 and 16 to correct for instrumentation errors.

In an attempt to determine the effect of explosion depths upon the pressure pulse characteristics, Y, it was assumed that Y was proportional to the product of two functions of independent variables: a function of only the total charge depth, Z_o, and a function of only reduced range, $R/W^{1/3}$. The latter function had been determined by the principles of similitude from shallow water explosions and is assumed to be valid for all depths. The relationship is:

$$Y = g(Z_o)\ f\ (R/W^{1/3}) \qquad (4.1)$$

where Y is pressure, reduced impulse, $I/W^{1/3}$, reduced energy, $E/W^{1/3}$, or a reduced time interval between characteristic points in the pulse, $\tau/W^{1/3}$, and where Z_o = charge depth + 33 ft, R is range, and W is charge weight. By assuming power laws for g of a form similar to that used for f (reference 10), equation (4.1) becomes:

$$Y = k \cdot Z_o^{\alpha} \cdot (R/W^{1/3})^{\beta} \qquad (4.2)$$

where β is a constant determined empirically from shallow water explosions, and where k and α are constants determined by the method of least squares from the measured values of Y, Z_o, and $(R/W^{1/3})$. The results are shown in Table III and discussed below.

The relaxation (hysteretic) effect of the hydrophone used results in a lag (see footnote page 4) in the response to a decaying pressure so that, for example, positive pressures may still be recorded after the explosion pressures have entered the negative phase. The magnitude of this distortion increases with increase in the shock wave peak pressure level. Hence, for the smaller reduced ranges, all data recorded subsequent to the shock wave peak pressure (except the bubble periods) were affected. This is apparent in the graphs shown. Since the relationship between the magnitude of this distortion and the pressure level is not known, a criterion was adopted arbitrarily to eliminate from the least squares determination all data (except the bubble periods and shock wave peak pressures) recorded at reduced ranges less than about 500 ft/lb$^{1/3}$ (15-20 psi).

4.1 RESULTS FOR TNT

The results reported here are compared with similar earlier data obtained by NOL in 1949, 1963, and 1964 and reported by Blaik and Christian (reference 8). In addition, some shallow, long-range shots reported by Arons (reference 3) and some short-range bubble data (references 15 and 16) are compared.

4.1.1 TNT Pressures. The first positive phase (shock wave) peak pressures, P_{pp}, are plotted for TNT in Figure 4 for reduced ranges of $R/W^{1/3}$ between 200 and 14,000 ft/lb$^{1/3}$. A least squares fit to these data showed that the pressures varied as the reduced range, $R/W^{1/3}$, to the -1.13 power, as was determined by Arons (reference 3) from long-range, shallow-water explosions, by Blaik and Christian (reference 8) from long-range, deep explosions, by Vanzant and DeHart (reference 4) from short-range simulated deep explosions, and by Bebb and by Coles, et al (references 1 and 2) from short-range shallow water explosions. The pressures of references 1, 2, 3, 4, and 8 were only about 4% to 8% larger than the present peak pressures, and for clarity were omitted from Figure 4. In general, the peak pressure, from the 1-lb charges were lower than those from the 8-lb and 57-lb charges. All peak pressures were read from the apparent peaks; i.e., without correction for the finite gauge size and the 20 kHz recording response. This may account for the slightly lower peak pressures, particularly those for the 1-lb charges.

A similar plot of the first bubble pulse maximum pressures, P_B, against $R/W^{1/3}$ shows that the pressures were slightly depth dependent, as was indicated by a slight but significant increase in the slope of the curve at a reduced range of about 4000 ft/lb$^{1/3}$. This effect was not observed in reference 8, probably because the TNT measurements were made from explosions confined to depths greater than 4000 ft; i.e., 6000 to 22,000 ft, and because the scatter in the data was large. If it is assumed that the bubble peak pressures can be represented by simple power laws involving depth as well as the similitude requirements of charge weight and range (i.e., as in Equation 4.2) it can be shown by using the method of least squares, that $k = 3300$ and α is essentially zero; i.e., independent of depth, for depths less than about 4000 ft. For larger depths, however, a significant increase in P_B was observed with increase in charge depth: $\alpha = 1/6$ when $\beta = -1.00$. This is shown in Figure 5 where $P_B(R/W^{1/3})$ is plotted against Z_o. Reference 8 data (not shown) for 1- and 8-lb TNT charges fired between 6000 and 22,000 ft depths are in good general agreement with our data.

A comparison of bubble pressures from 1-lb TNT charges fired at 512-ft depth (reference 15) and at reduced ranges of 2.85 and 5.69 ft/lb$^{1/3}$, shows reference 15 pressures to be about 5% smaller than ours. Approximately the same difference was found with reference 16 results for 500- and 250-ft depths at a reduced range of 2.84 ft/lb$^{1/3}$.

From an incompressive approximation of the pulsating bubble, Arons derived the following expression (reference 16) for the minimum pressure of the first bubble negative phase:

$$P_{min} = -5.16\, Z_o^{2/3}\, (R/W^{1/3})^{-1.00} \qquad (4.3)$$

By assuming our pressures also to vary inversely with the reduced range, the effect of charge depth upon the pressure is shown in Figure 6 by plotting $P_{min}(R/W^{1/3})$ against Z_o. From a least squares fit to the data for $Z_o < 4500$ ft, the pressure varied as the total charge depth, Z_o, to the 2/3 power, as was determined by Arons. The absolute pressure level computed from Arons' equation (4.3) was about 7% larger than ours.

Below 4500 ft, however, a change in slope occurs, and the negative pressures vary as depth to the 1/3 power. Interestingly enough, the reference 8 pressures, when plotted on the Figure 6 scales, do not show this change in slope.

4.1.2 TNT Impulses. The first positive phase impulse, I_{pp}, was reduced by the factor $(W^{1/3}/Z_o^{1/3})$ and is shown plotted against reduced range in the lower graph of Figure 7. The exponent of Z_o was determined by applying least square fits to the data in Equation 4.2 where $Y = I_{pp}/W^{1/3}$ and $\beta = -0.97$.

Additional unreported data were obtained by NOL from a 1.8-lb TNT charge fired in the Pacific (reference 19) at 865-ft depth and measured at a horizontal range of about 8400-ft and 1500-ft depth. The transmission characteristics were such that the pulse was not refracted, and the reduced impulse of the first positive phase is shown in Figure 7 to be in good agreement with our data for a reduced range of 6900 $ft/lb^{1/3}$. Also shown are the reference 8 first positive phase impulses from 1-lb and 8-lb TNT charges fired at depths of 6000-22,000 ft. They average about 25% higher than the values reported here.

The insert at the bottom of Figure 7 shows the reference 4 first positive phase impulses obtained from 8.5 and 14.8 gram pentolite charges fired in a fresh water filled tank pressurized to simulate ocean depths of 1150 to 9000 ft. The impulses are about 25% higher than our data for TNT extrapolated to reduced ranges of 1-10 $ft/lb^{1/3}$.

Reference 3 shallow water ($Z_o \approx 75$ ft) shock wave impulses were measured from 1/2-lb pentolite charges at reduced ranges from 100 to 1000 $ft/lb^{1/3}$. Adjustment of this data to include the impulse in the entire positive phase (reference 18) results in very good agreement with our curve in Figure 7.

The first bubble pulse impulse was reduced by the factor $(W^{1/3}/Z_o^{2/5})$ and is shown plotted against reduced range in the upper graph of Figure 7. The exponent of Z_o was similarly determined from Equation 4.2; however, in this case, the value of β was assumed to be -1.00. Reference 8 first bubble pulse reduced impulses are also plotted in Figure 7. An extrapolation of our curve to the large reduced ranges shows reference 8 values to be about 20% larger than our impulses. Reference 16 gives values of bubble impulses measured at a very small reduced range from TNT charges fired at about 500-ft and 250-ft depths. Extrapolating the impulse curve for our data to this reduced range of 2.84 $ft/lb^{1/3}$ gives impulse values equal to the reference 16 impulses. A similar comparison with reference 15 impulses is almost equally good for a 512-ft charge depth and reduced ranges of 2.84 and 5.69 $ft/lb^{1/3}$.

The bubble impulse and the bubble maximum pressure were calculated for a 1-lb charge for $Z_o = R + 210$ ft from Arons' incompressible bubble theory (reference 17). The calculated impulses were within 15% of our curve for reduced ranges less than 10,000 $ft/lb^{1/3}$, and a similar deviation was obtained for the calculated bubble pressures for reduced ranges less than 4,000 $ft/lb^{1/3}$.

4.1.3 TNT Energy Flux Densities. The energy, E_{pp}, in the first positive phase for TNT (as well as HBX-3) is shown in Figure 8. The data were reduced by the factor $W^{1/3}/Z_o^{1/5}$; the exponent of Z_o was determined by a least squares fit to Equation 4.2 with exponent β taken as -2.07. The energies of reference 8 are shown for comparison; they are about 25% higher than the corresponding values of this report.

Also shown in Figure 8 is an unreported energy value of the first positive phase measured at a reduced range of 6900 $ft/lb^{1/3}$ (reference 19). This value is in good agreement with our data. The reference 3 shock wave energies averaged about 10% less than our curve in Figure 8 for reduced ranges between 100 and 1000 $ft/lb^{1/3}$. No energy values were reported in reference 4.

4.1.4 TNT Pulse Durations. Figure 2 shows the notations used for the various pulse durations. Figures 9 and 10 show how the durations of the various phases of the pressure pulse through the first bubble positive phase vary with Z_o, the total charge depth. (The shock wave rise times are not included here, since the slow response of the recording and playback system masked the true rise times. The actual rise times are less than the 55 ± 5 microseconds recorded on all shots.) As a result of the hydrophone relaxation effect, the recorded values of τ_{NP} were too small and the recorded durations of τ_{PP}, τ_{BRT}, and τ_{BPP} were too large at the smaller reduced ranges.

These figures show that the reduced first bubble period, $\tau_1/W^{1/3}$, and the reduced duration of the first bubble negative phase, $\tau_{NP}/W^{1/3}$, varied as the total charge depth to the -5/6 power for all explosion depths between 500 and 15,000 ft. The equation for $\tau_{NP}/W^{1/3}$ in reference 8 obtained for 1- and 8-lb TNT charges for charge depths from 6500 to 22,000 ft is identical to that reported here. Also the equation for $\tau_1/W^{1/3}$ is in good agreement with values reported in references 5, 8, 15, and 16 for non-migrating TNT bubbles.

The reduced duration of the first bubble rise time, $\tau_{BRT}/W^{1/3}$, varied as the -0.93 power of Z_o over the entire range of depths (Figure 10); however, because of the short durations at the greater depths, the precision of measurement is only fair.

The reduced durations of the first positive phase, $\tau_{PP}/W^{1/3}$, and of the first bubble phase, $\tau_{BPP}/W^{1/3}$, also varied as the total charge depth to the -5/6 power, but only for charge depths less than about 4500 ft. For larger depths, a significant departure from the -5/6 slope was observed for these two durations. The curves drawn by eye through the cluster of durations for explosion depths of 4500, 7000, and 14,000 ft show a slope of -2/5 for $\tau_{PP}/W^{1/3}$, and -3/5 for $\tau_{BPP}/W^{1/3}$. The corresponding reduced durations* of references 6 and 8 in the depth interval of 6000-22,000 ft are in good agreement. It should be noted that 4500 ft is the depth for which significant changes in the first bubble pressures occurred.

Shallow water (Z_o = 75 ft) shock wave time constants were shown in reference 3 to increase with increase in reduced range at a rate $(R/W^{1/3})^{0.22}$ for reduced ranges as large as 2000 ft/lb$^{1/3}$. Our reduced time constants** ($\theta/W^{1/3}$), however, were independent of reduced range; the measured values, after correction for the 20 kHz response, were 170, 160, and 150 microsec/lb$^{1/3}$ for the 1-, 8-, and 57-lb TNT charges, respectively, in the reduced range interval of 500 to 14,000 ft/lb$^{1/3}$. The spreading of the profile (reference 3) with increase in range is apparently counteracted by a compression of the profile with increase in charge depth. This can be shown from Equation 4.2, where a selection of a reasonable value for β results in α being the negative of that value. The best fit to our data is obtained when $-\alpha = \beta \approx 0.10$.

Equation 4.2 and what little other data was reported (reference 18 and 19) were used to determine the effect of reduced range upon the durations of the first positive phase, τ_{PP}. The effect was negligible: β was less than 0.05 when α was assumed to be -5/6. However, as more data become available, especially measurements at

* Some durations in Figures 9 and 10 are not reported in references 6 and 8 but were specially read for inclusion in this report.

** The time constant is defined as the time required for the peak pressure to decay to 36.8% of its peak value, as for exponential pulses, although our pulses approach a linear decay for the very large depths.

depths about equal to the charge depths, a better determination of the charge range and depth dependence will be obtained.

4.2 RESULTS FOR HBX-3

Table I lists the HBX-3 shots fired. Although the shallowest shot was at 1200 ft, the reduced ranges varied from 500 to 14,000 ft/lb$^{1/3}$. No earlier deep HBX-3 data are available, so comparisons are made only with shallow explosion data, and one set of close-in measurements made at 500-ft depth.

4.2.1 HBX-3 Pressures. In Figure 11, the HBX-3 first positive phase (shock wave) peak pressures are plotted against reduced range ($R/W^{1/3}$) between 500 and 14,000 (ft/lb$^{1/3}$). A least squares fit* to the data shows that a slope of -1.14 is maintained to 14,000-ft depths. The same value of slope was reported in reference 20 from several series of HBX-3 charges fired at reduced ranges of only 1.65 to 21.5 ft/lb$^{1/3}$ at about a 30-ft depth. The line of Figure 12 was extrapolated to these short ranges and the reference 20 values were found to lie about 2% below the line.

The peak pressures found here were 3 to 7% smaller than those for TNT at the corresponding ranges. This is slightly smaller than the results of shallow-water, short-range measurements, as summarized in reference 21. There, the peak pressure of HBX-3 averaged 3% higher than that of TNT.

As in the case of TNT, the first bubble maximum pressure, P_B, can be expressed by Equation 4.2. If β is assumed to be -1.00, the method of least squares applied to the data gives k = 2100 and α essentially zero (independent of charge depth) for Z_o less than about 4000 ft. For $Z_o > 4000$ ft, however, the pressure increases with increase in charge depth and $\alpha = 0.15$ when $\beta = -1.00$. This is shown in Figure 12 where $P_B \cdot (R/W^{1/3})$ is plotted against Z_o.

Reference 15 reports bubble maximum pressures from 1-lb HBX-3 charges fired at a 512-ft depth and reduced ranges of 2.85 and 5.69 ft/lb$^{1/3}$. The reference 15 pressures were about 5% smaller than our values obtained from the appropriate equation in Table III for the above reduced ranges. While the absolute values differ, the ratio of the first bubble maximum pressures for TNT to those for HBX-3 is essentially the same here (0.62) and in reference 15 (0.64).

The effect of depth upon the first bubble minimum pressure, P_{min}, was determined from Equation 4.2, with $\beta = -1.0$. In Figure 13, the pressure, reduced by ($W^{1/3}/R$), is plotted against Z_o. A least squares fit to the data for $Z_o \geq 3000$ ft gives 1/2 for the exponent of Z_o and -16.5 for the proportionality constant k. At the shallower depths, the scatter is too great and the data too few to fit a line as was done for TNT in Figure 6. However, if the two 8-lb and one 50-lb data points were eliminated because of relaxation effects, an extension of the curve (dashed line) would provide a good fit to the remaining data including that from reference 15.

4.2.2 HBX-3 Impulses. In Figure 14, the HBX-3 first positive phase impulse, reduced by $(W/Z_o)^{1/3}$, is plotted against reduced range between values of 400 and 14,000 ft/lb$^{1/3}$. The parameters k and α were determined from Equation 4.2 assuming an exponent of -0.97 for the reduced range; these are shown in Table III.

* The very small pressures at $R/W^{1/3} = 2550$ and 3400 were not used in this or other determinations since all pressure characteristics for these two shots were systematically low.

The impulse values found here were about 22% greater than those for TNT at the corresponding conditions. This is consistent with the short range data which averaged 24% greater (reference 21). When the line in Figure 14 is extrapolated to the short ranges and shallow depths for which the impulse equation in reference 20 applied, the agreement is to within a few percent if the differences in impulse due to integration times are taken into account.

The impulse of the first bubble positive phase, I_B, reduced by $W^{1/3}/Z_o^{2/5}$, is also plotted in Figure 14 against reduced range. Again, k and α were obtained from Equation 4.2, assuming $\beta = -1.00$, and are given in Table III. This line was extrapolated to the very short ranges (2.85 and 5.69 ft/lb$^{1/3}$) of the reference 15 shots fired at 512-ft depth. Even at this great extrapolation, the reference 15 impulses were only 3% higher than our values.

It is interesting to note that while the HBX-3 bubble pulse impulse is about 20% greater than the TNT values, the HBX-3 bubble pulse maximum pressures are only about 2/3 of the TNT values. This is because the positive duration of the HBX-3 bubble pulse is much greater than that of TNT. The 20% difference between TNT and HBX-3 bubble pulse impulses found here can be compared with the 30% difference reported in reference 15.

4.2.3 HBX-3 Energy Flux Densities. The reduced energy of the first positive phase for HBX-3 plotted against reduced range is shown in Figure 8, which also shows the TNT energy. As done for TNT, the best fit to Equation 4.2 was one in which the HBX-3 energy was reduced by $(W^{1/3}/Z_o^{1/5})$. However, in this case the exponent of the reduced range was assumed to be -2.04.

A comparison of the HBX-3 and TNT energies obtained in this study shows that the HBX-3 energies are 10% to 20% larger than the TNT energies at depths between 500 and 10,000 ft. Reference 21 gives for short range shallow data a value for HBX-3 of 1.28 relative to TNT.

The line of Figure 8 was extrapolated to the short ranges and shallow depths where the equation for energy given in reference 20 is applicable; the reference 20 values were all 0-10% below the line.

4.2.4 HBX-3 Pulse Durations. Reduced pulse durations are shown in Figures 15 and 16 as functions of depth*.

The range of depths is not as large as that for TNT and considerably fewer data were obtained. However, the scatter in the data for the first bubble period, τ_1, and for the duration of the negative phase τ_{NP}, was small and a least squares fit provided a slope of -5/6 down to depths of 10,000 ft. The first bubble period coefficient of 5.35 was 2.4% less than the reference 15 value obtained from 1-lb charges detonated at a 512-ft depth.

The reduced values of the first positive phase τ_{PP} and the bubble positive phase duration τ_{BPP} also varied as $Z_o^{-5/6}$ for depths down to about 5000 ft. For depths

* Three pressure-time records were obtained from 14,000-ft HBX-3 shots. However, for lack of sonic ranging data, the depths for these three values were determined from the experimental bubble period equation. The depths thus calculated were used only with the τ_{PP}, τ_{BRT}, and τ_{BPP} data.

greater than 5000 ft, a departure from this slope was observed similar to that for TNT; the absolute magnitudes of the slopes were slightly larger than the corresponding ones for TNT.

As was the case for TNT, a straight line was drawn through the reduced bubble rise time data τ_{BRT} between 1200 and 14,000-ft depths; a slope of 0.90 was obtained. The HBX-3 bubble pulse rise times were 58% to 70% greater than the TNT rise times.

The increase in time constant with increase in range was again counteracted by a corresponding decrease with increase in depth; the reduced time constants were independent of depth and range and were 200, 182, and 182 microsec/lb$^{1/3}$ for the 1-, 8-, and 50-lb charges, respectively.

4.3 NITRAMEX AND PENTOLITE

Nitramex and Pentolite pressure pulse measurements are included in Table II. No graphs and equations are presented since only four 80-lb Nitramex charges were fired at depths between 2800 and 10,300 ft and only three 1-lb Pentolite charges were fired between 550- and 6600-ft depths. The results of these shots are compared with the TNT results at corresponding conditions. Since the scatter in the Nitramex data is large, the Nitramex results are not considered reliable.

4.3.1 Nitramex Comparison with TNT. The values of the Nitramex shock wave and bubble pulse characteristics are, in general, considerably smaller than those for TNT. The first positive phase peak pressures averaged about 70% of the TNT pressures and the first bubble peak pressures averaged about 60% of the corresponding TNT pressures. The absolute value of the bubble minimum pressure averaged about 70% of the TNT pressure. The first positive phase impulse and the first bubble impulse were comparable to the TNT values at the shorter ranges; at the greater ranges, they were 75% and 60% of the corresponding TNT impulses. The energy in the first positive phase averaged 55% of the TNT energy for the longer ranges and was comparable for the shorter reduced ranges. The Nitramex reduced durations, however, are in fair agreement with the corresponding TNT values; in general, the Nitramex reduced durations fall within the scatter of the TNT data, τ_{BRT} being slightly higher and τ_{BNT} slightly lower. The average value of the first bubble period coefficient, K_1, was about 4.24, or 2.3% less than for TNT.

4.3.2 Pentolite Comparison with TNT. The three values of Pentolite first positive phase peak pressure are in very good agreement with the shallow water Pentolite and TNT data of reference 3. The three data points are within the scatter of our TNT data, and no significant difference can be obtained. (Reference 21 gives Pentolite as having an 8% higher value than TNT at short ranges.) The Pentolite bubble maximum pressure, both impulses, and the first positive phase energy were roughly 25% greater than the corresponding 1-lb TNT data. All reduced durations were within the scatter of the TNT plots, and the average value of the first period coefficient, K_1, was 4.40. The reference 5 value of K_1 was 4.47 for 6000-ft depths.

5. SUMMARY AND CONCLUSIONS

An attempt has been made to determine the effects of reduced range and of the depth of an explosion upon the pressure pulse characteristics from data measured at ranges nearly equal to the charge depths. The following equation was used for each pressure pulse characteristic:

$$Y = k\, Z_o^{\alpha} (R/W^{1/3})^{\beta}$$

The similitude scaling laws of reduced range for shallow water explosions were used to find the parameters for all depths of explosion. The parameters in the above equation and the limits of the independent variables are given in Table III for each pressure pulse characteristic measured. In general, good agreement was obtained by extrapolating the characteristics dependent on depth and reduced range to corresponding data obtained from shallow water explosions at short and long ranges, from short range measurements at intermediate and large depths and for an isolated case of intermediate charge depth and long range. However, for a better check on the validity of the relationships developed for the dependence on depth and reduced range, pressure measurements are required from deep and intermediate depth explosions at short and intermediate ranges.

Some conclusions drawn from this analysis show that within the precision of the measurements, only the shock wave peak pressures, P_{pp}, were independent of depth and only the pulse durations were independent of reduced range. The absolute magnitudes of the bubble minimum pressure, P_{min}, and of the bubble peak pressure, P_B, (only for $Z_o > 4000$ ft) increased with increase in depth; all other characteristics measured decreased with increase in depth. Of all the depth-dependent characteristics, the effect of depth was greatest upon the first bubble rise times and least upon the first bubble peak pressure. However, the effect was great upon the other pulse durations and upon the bubble minimum pressure. At a depth of about 4500 ft, a change occurs in the effect of depth upon the bubble minimum and peak pressures, and upon the durations of the first positive phase and of the first bubble positive phase. The effect of depth counteracts that of the reduced range so that the shock wave "time constants" are constant for all depths and reduced ranges for this case where $Z_o \approx R + 210$. Comparisons of the HBX-3 pressure pulse characteristics with those of TNT were in good general agreement with similar comparisons made in shallow water, and at a 500-ft depth.

REFERENCES

1. A. H. Bebb, "Measurement of Pressure, Momentum and Energy from Underwater Explosive Charges at Ranges from 100 to 1 Charge Radii", British Report NCRE/R 150, UNDEX 264, Nov 1951, Unclassified.

2. J. S. Coles, et al, "Shock Wave Parameters from Spherical HBX and TNT Charges Detonated Under Water", NAVORD Report 103-46, Dec 1946, Unclassified.

3. A. B. Arons, "Underwater Explosion Shock Wave Parameters at Large Distances from the Charge", J. Acoust. Soc. Am. 26, 343-346, 1954.

4. B. W. Vanzant and R. C. DeHart, "Effect of Hydrostatic Pressure on Shock Waves from Underwater Explosions", J. Appl. Phys. 36, 3116-3117, 1965; and "Shock Characteristics of Small Pentolite Charges Detonated in Vessels Hydrostatically Pressured from Ambient to 4000 psi", Southwest Research Inst. Final Report, Contract No. Nonr-3940(00), Project 03-1284, Sep 1965, Unclassified.

5. John P. Slifko, "Studies of Explosions at Depths Greater than One Mile in the Ocean, VI. Bubble Period Measurements", NAVORD Report 2276, Aug 1954, Unclassified.

6. W. H. Faux and C. R. Niffenegger, "The Resistance of Hollow Glass Models to Underwater Explosions at Great Depths I. Spheres", NOLTR 65-145, Dec 1965, Unclassified.

7. W. H. Faux, "The Resistance of Hollow Glass Models to Underwater Explosions at Great Depths II. Special Configurations", NOLTR 65-146, Jan 1966, Unclassified.

8. Maurice Blaik and Erwine A. Christian, "Near Surface Measurements of Deep Explosions I. Pressure Pulses from Small Charges", J. Acoust. Soc. Am. 38, 50-56, 1965.

9. C. R. Niffenegger, "Initiation of Mk 2 Mod 3 Demolition Charges", NOL Internal Memorandum TN 6989, Sep 1965, Unclassified.

10. R. H. Cole, "Underwater Explosions", Princeton University Press, Princeton, New Jersey, 1948.

11. D. J. Torpy, "A Transistorized High-Input Resistance Amplifier for Use with Piezoelectric Gages", NOL Internal Memorandum TN 6353, May 1964, Unclassified.

12. J. P. Slifko, "Evaluation of Hydrophones for Underwater Explosion Pressure Measurements", NOL Internal Memorandum, TN 7107, Jan 1966, Unclassified.

13. M. A. Genau, "Underwater Shock Wave Frequency Spectrum Analysis IV. Fortran IV Programs for the IBM 7090 Computer", NOLTR 66-3, Feb 1966, Unclassified.

14. M. A. Genau, "Spectrum and Octave Band Analysis of Pressure Pulses from Deep Underwater Explosions", NOLTR 66-128, Oct 1966, Unclassified.

15. Ermine A. Christian, Jean A. Goertner, J. P. Slifko, and E. Swift, Jr., "The Effect of Aluminum on Underwater Explosive Performance: Bubble Pulse Parameters from 1-lb Charges", NAVORD Report 2277, Jan 1952, Unclassified.

16. A. B. Arons, et al, "Measurement of Bubble Pulse Phenomena IV: Pressure-Time Measurements in Free Water", NAVORD Report 408, Nov 1947, Unclassified.

17. A. B. Arons, "Secondary Pressure Pulses Due to Gas Globe Oscillation in Underwater Explosions II. Selection of Adiabatic Parameters in the Theory of Oscillation", NAVORD Report 420, May 1948, Unclassified.

18. A. B. Arons and D. R. Yennie, "Energy Partition in Underwater Explosion Phenomena", NAVORD Report 406, Oct 1957, Unclassified.

19. E. A. Christian, C. R. Niffenegger, et al, "Explosive Echo Ranging Tests Against SQUAW-29; Preliminary Test Report (U)", NOLTR 61-126, Oct 1961, Confidential.

20. Alys R. Pittman and T. B. Heathcote, "Underwater Explosion Parameters for HBX-3", NAVORD Report 4167, Jun 1956, Confidential.

21. K. Caudle, Jean Goertner, N. Holland, "Explosives--Effects and Properties (U)", NOLTR 65-218, 21 Feb 1967, Confidential.

22. Ermine A. Christian and Maurice Blaik, "Near-Surface Measurements of Deep Explosions II. Energy Spectra of Small Charges". J. Acoust. Soc. Am. 38, 57-62, 1965.

23. D. E. Weston, "Underwater Explosions as Acoustic Sources", Proc. Phys. Soc. (London) LXXVI, 2, 233-249 (1960).

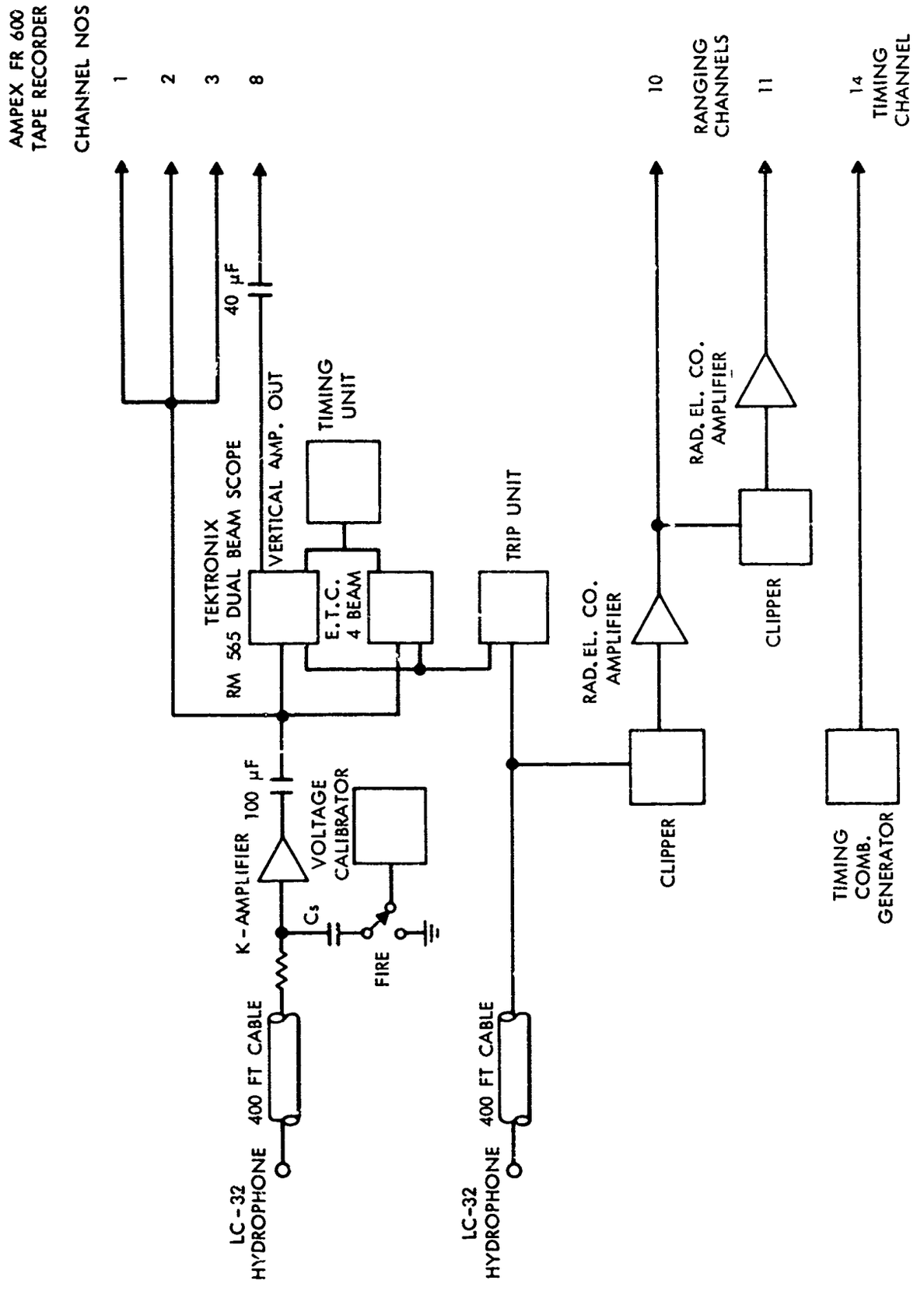

FIG. 1 BLOCK DIAGRAM OF PRESSURE-TIME RECORDING SYSTEM

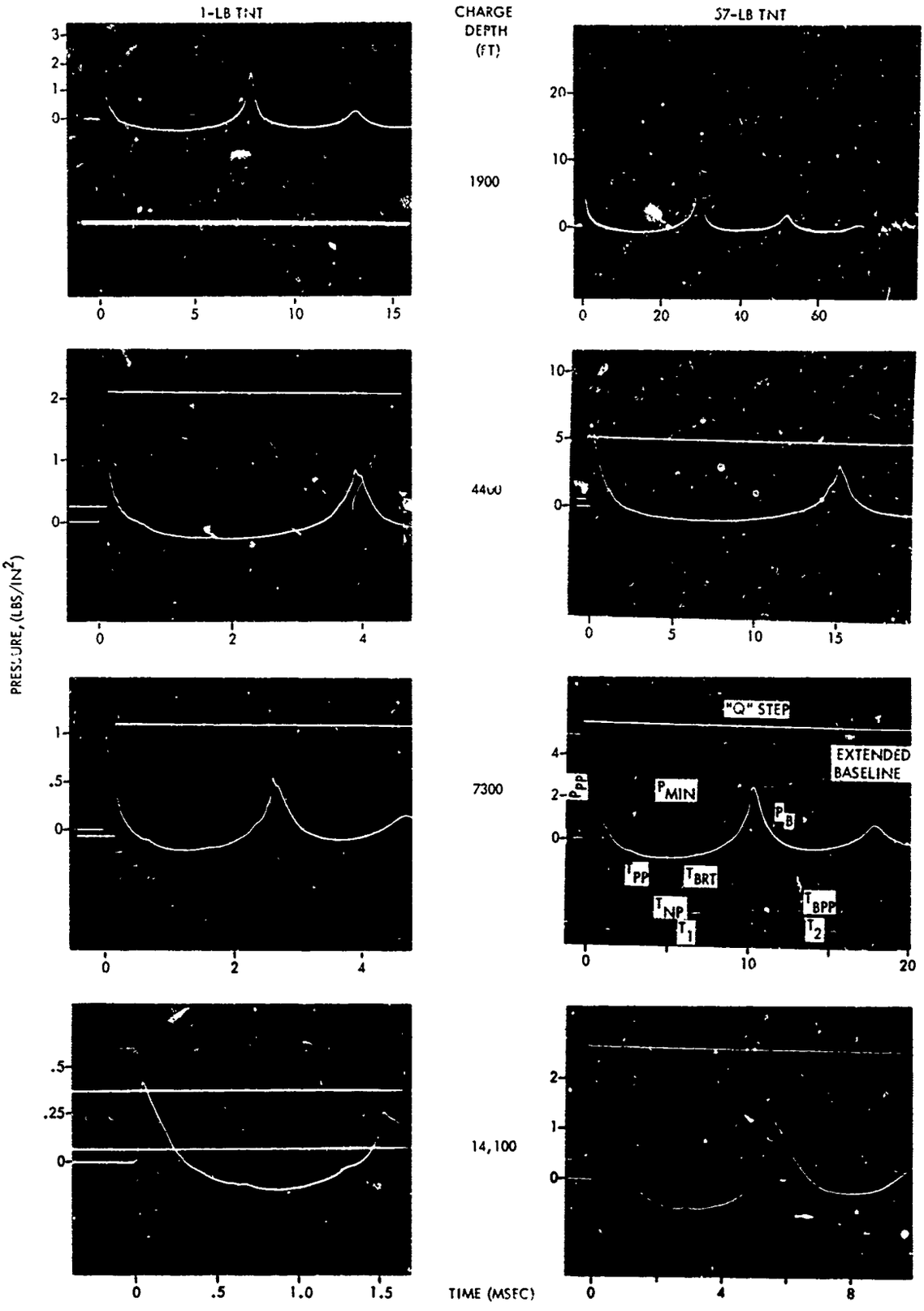

FIG. 2 TNT PRESSURE-TIME RECORDS FOR TWO WEIGHTS AND SEVERAL DEPTHS

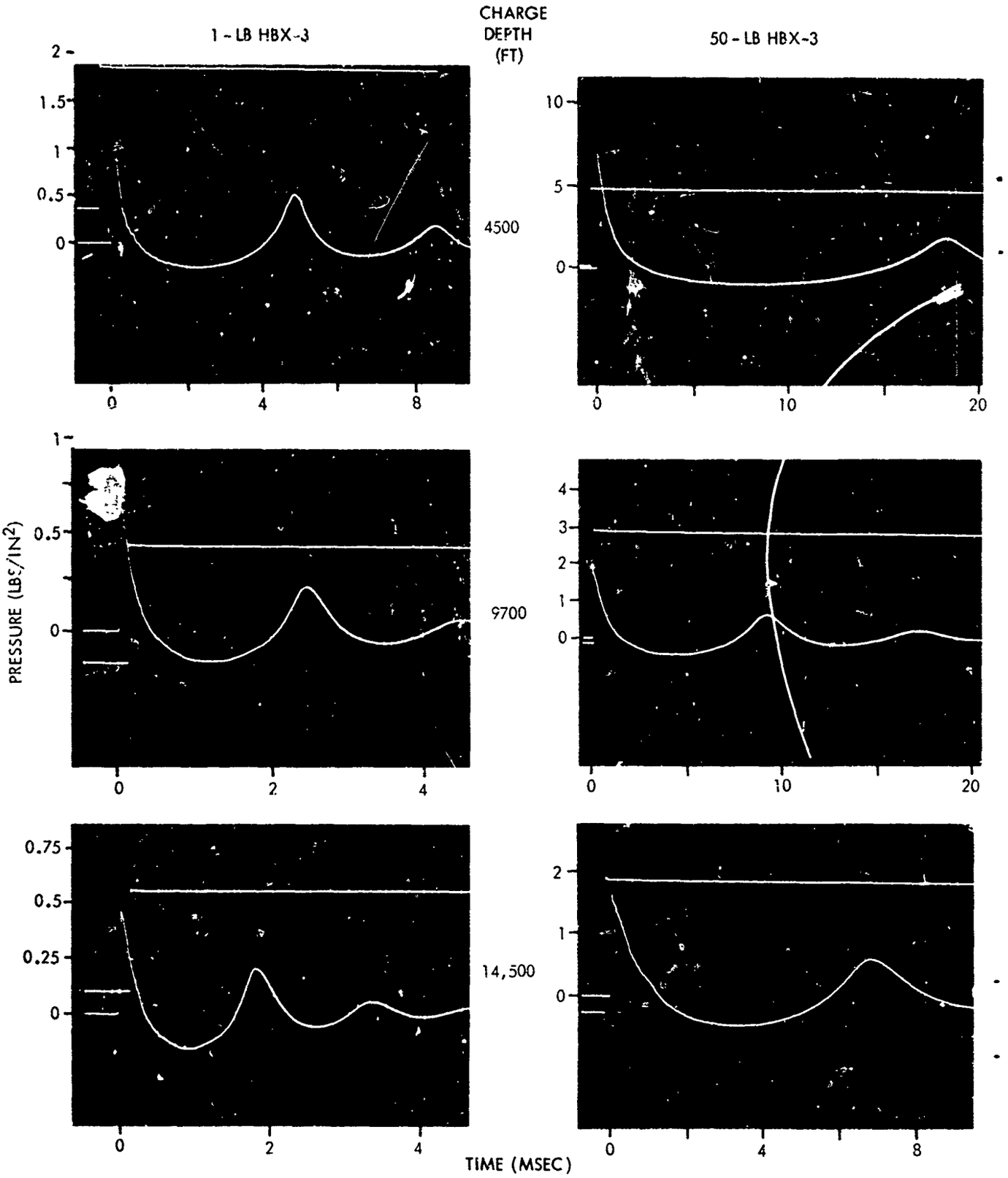

FIG. 3 HBX-3 PRESSURE-TIME RECORDS FOR TWO WEIGHTS AND SEVERAL DEPTHS

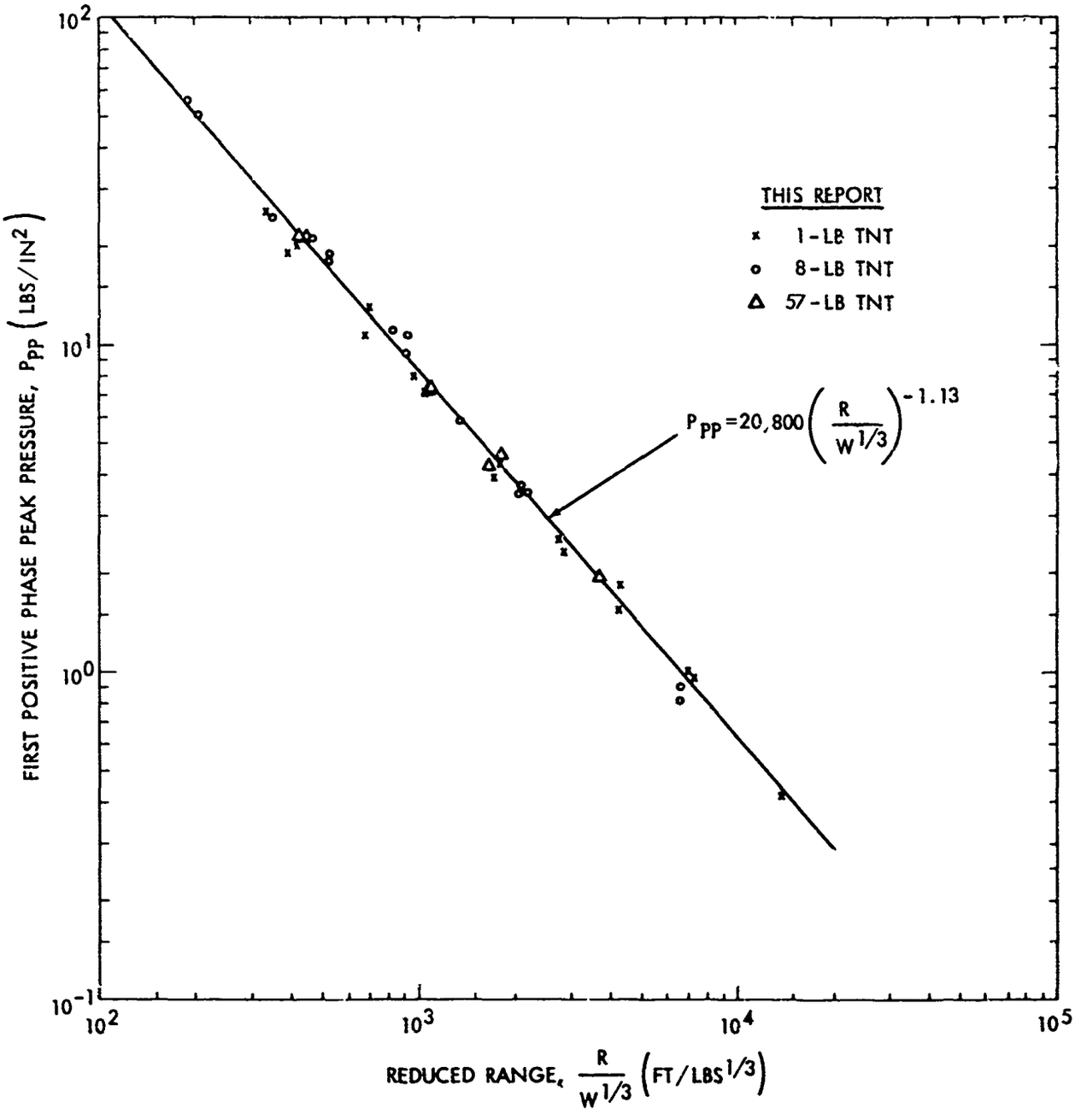

FIG. 4 P_{PP} VS $R/W^{1/3}$ FOR TNT

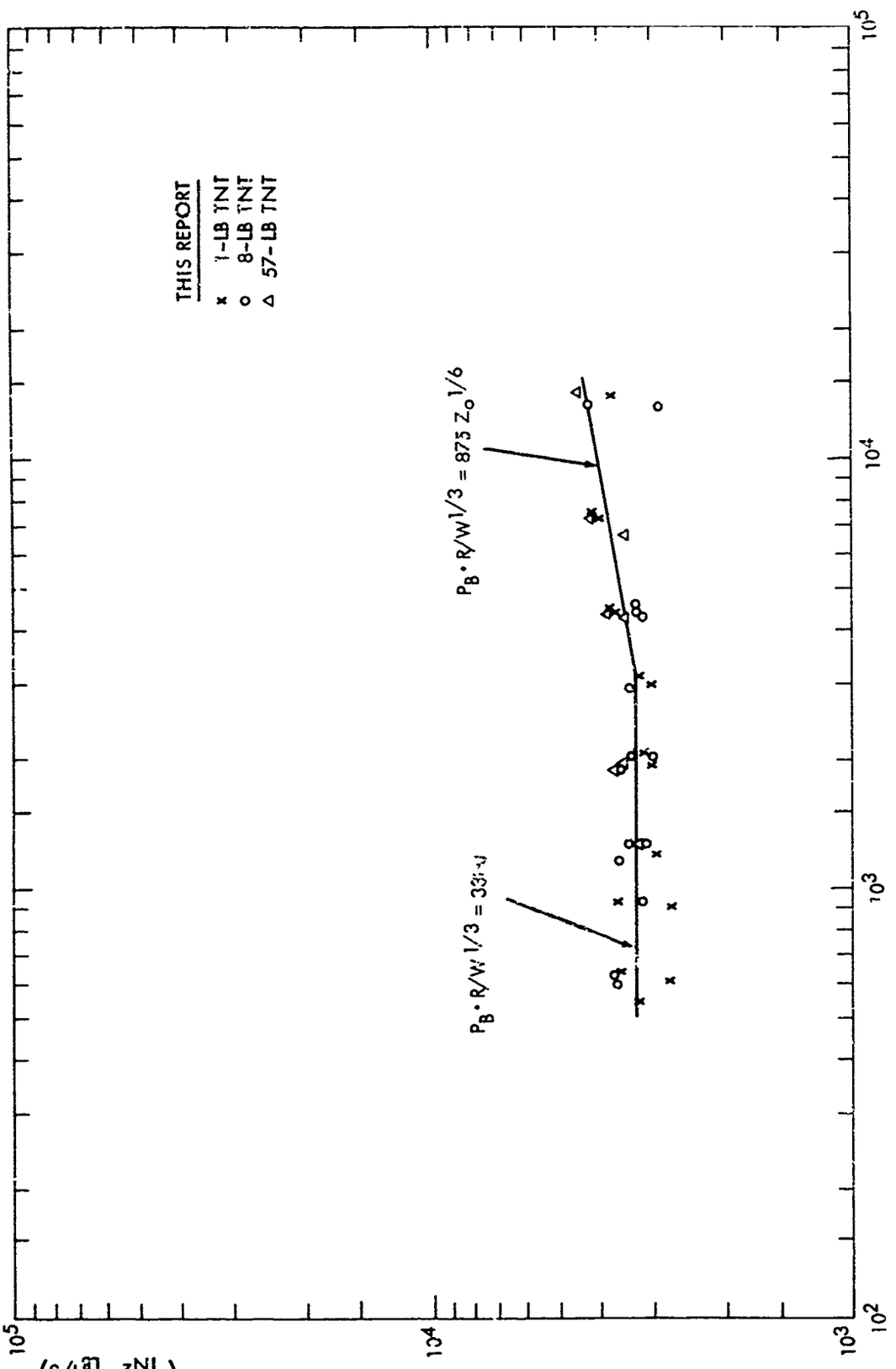

FIG. 5 $P_B \cdot R/W^{1/3}$ VS Z_o FOR TNT

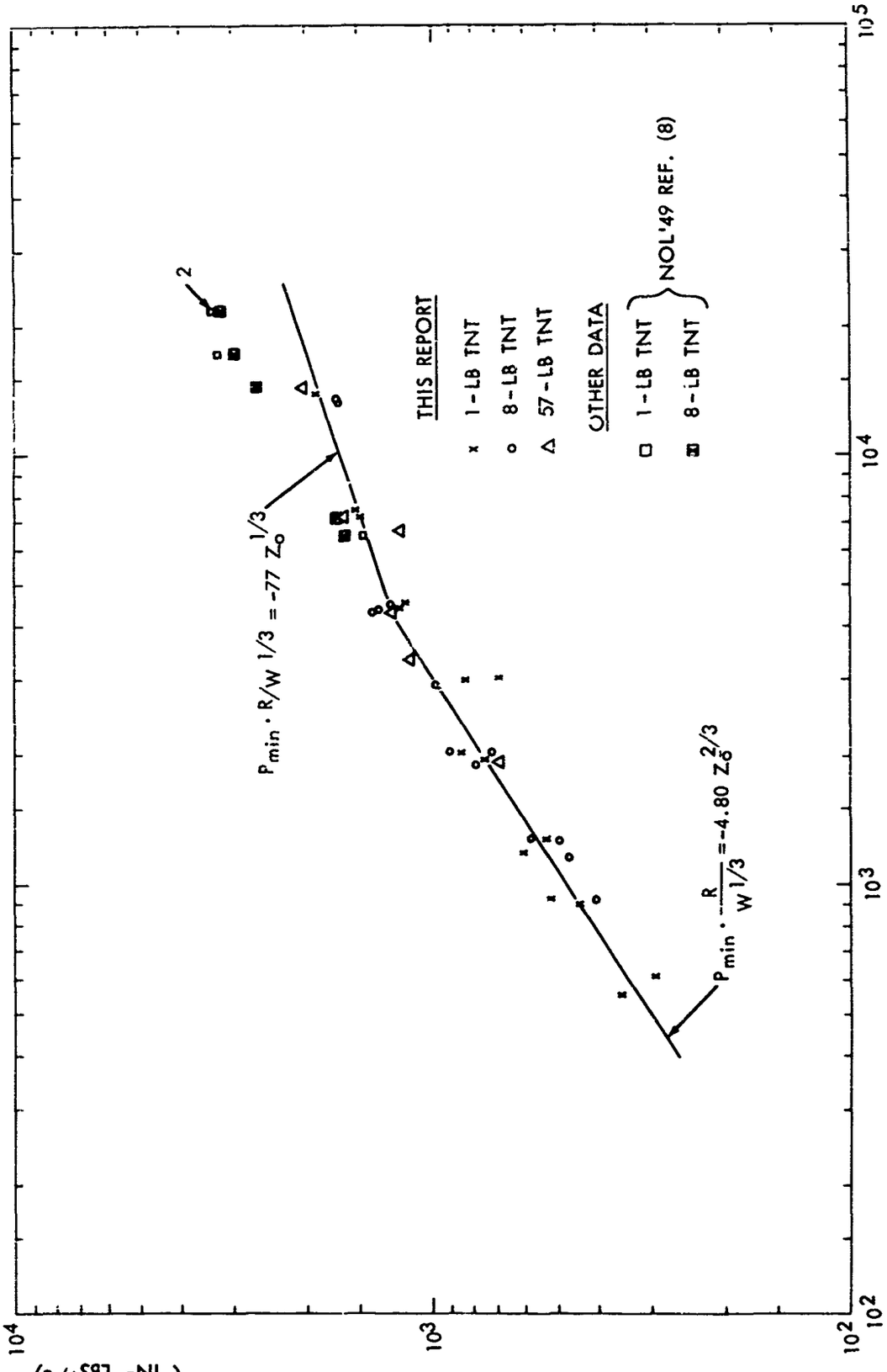

FIG. 6 $P_{min} R/W^{1/3}$ VS Z_o FOR TNT

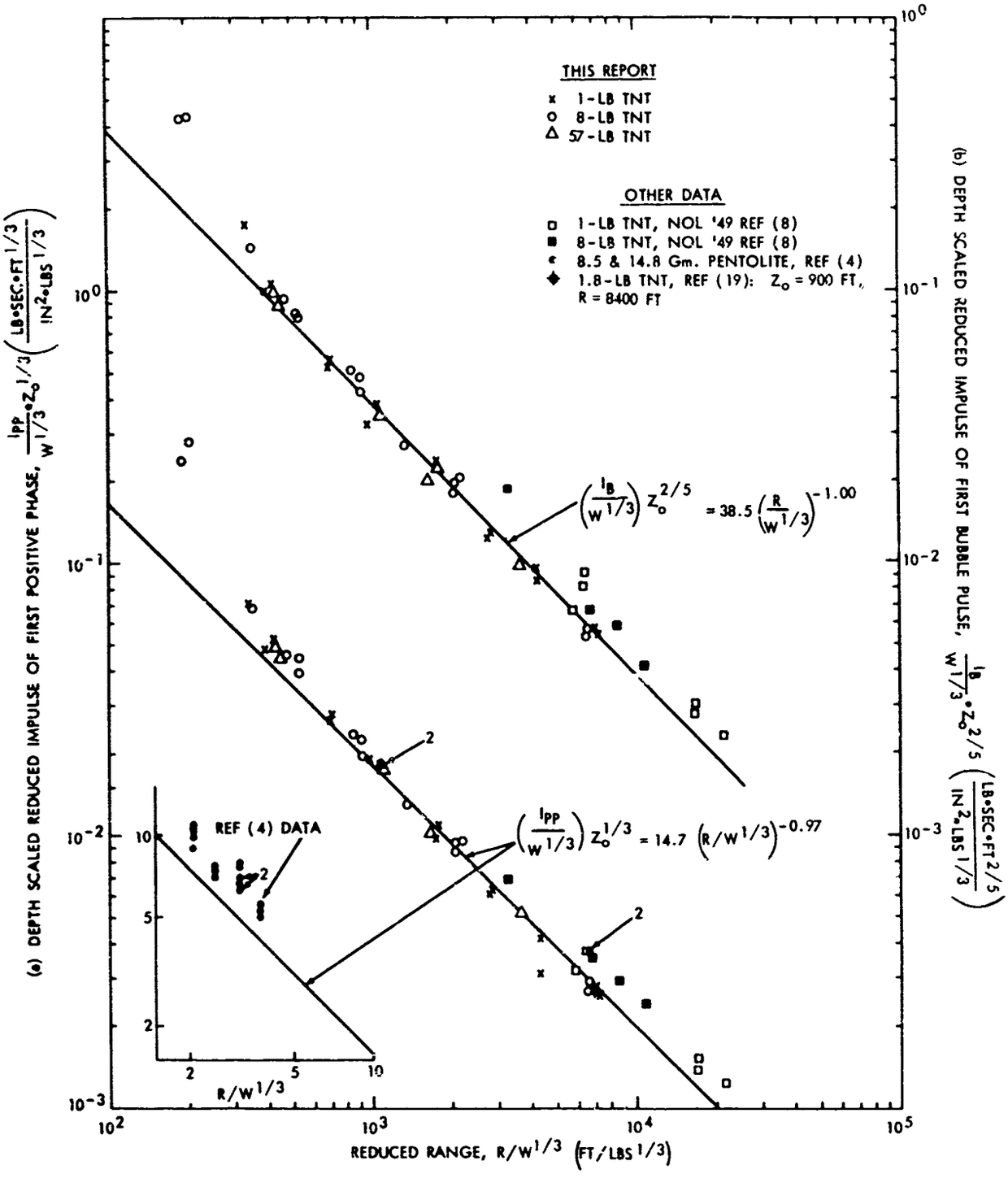

FIG. 7 (a) $I_{PP} Z_o^{1/3}/W^{1/3}$ VS $R/W^{1/3}$ FOR TNT
(b) $I_B Z_o^{2/5}/W^{1/3}$ VS $R/W^{1/3}$ FOR TNT

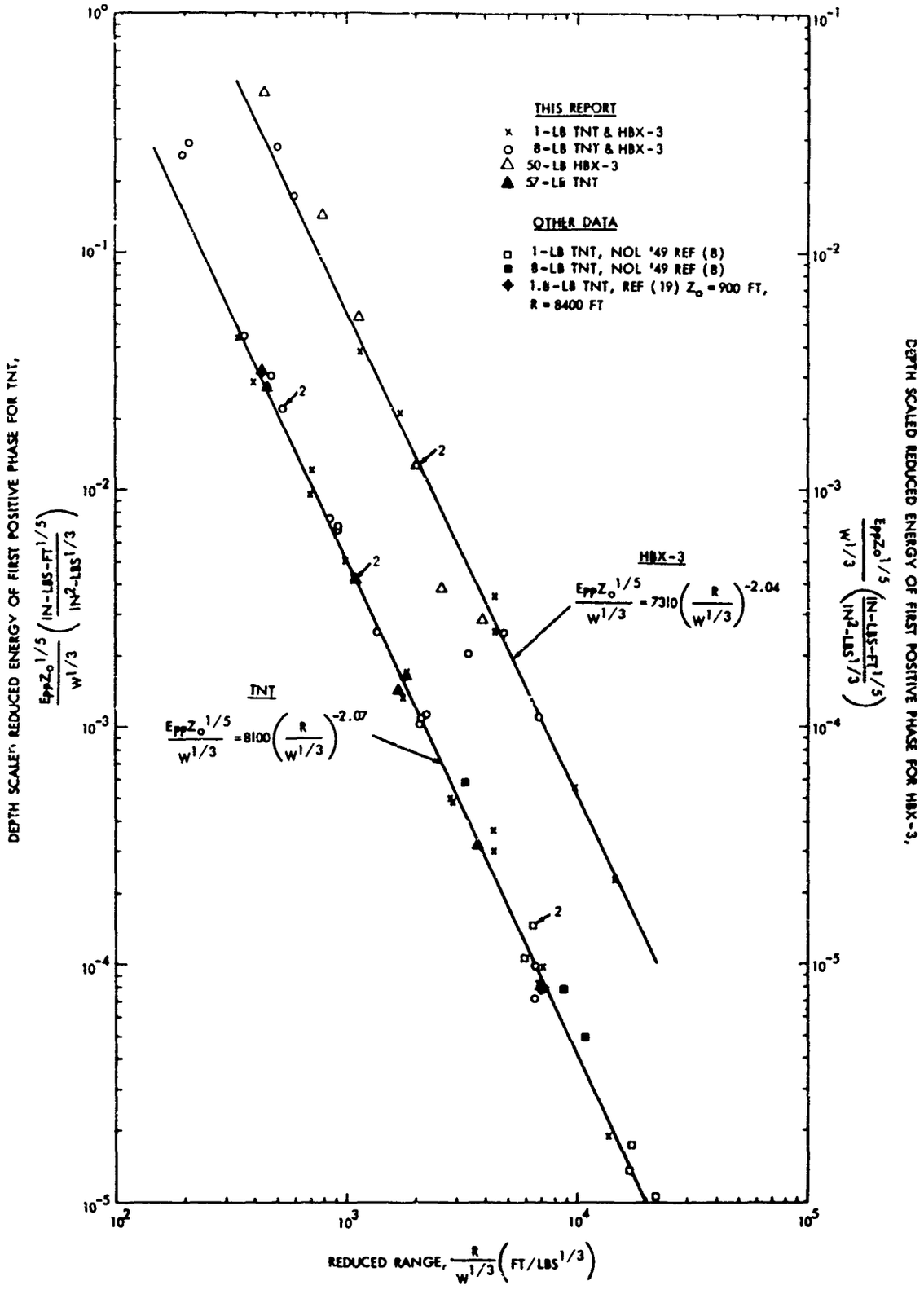

FIG. 8 $E_{pp} Z_o^{1/5}/W^{1/3}$ VS $R/W^{1/3}$ FOR TNT AND HBX-3

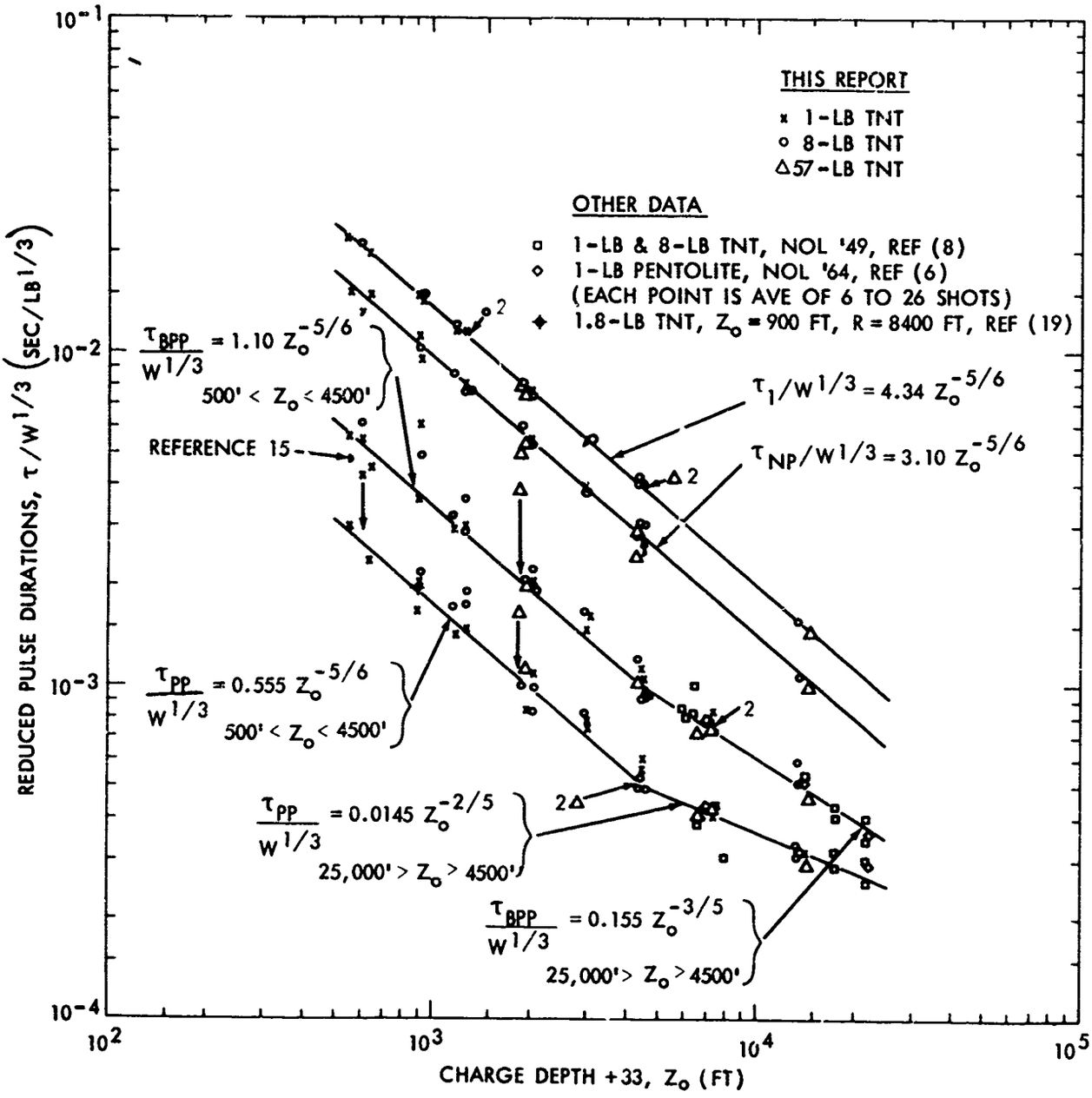

FIG. 9 REDUCED PRESSURE PULSE DURATIONS: $\tau/W^{1/3}$ VS Z_o FOR TNT

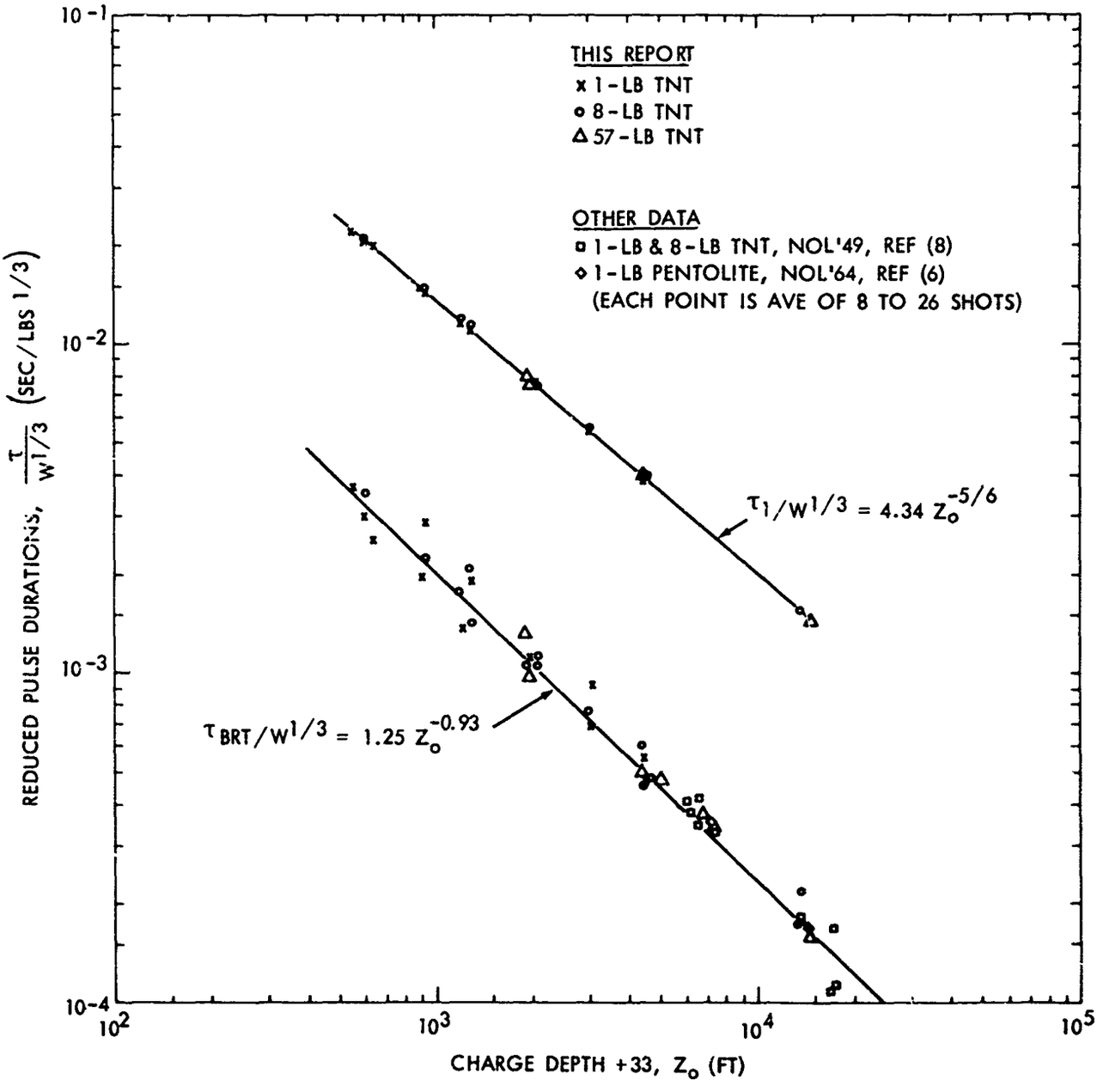

FIG. 10 REDUCED PRESSURE PULSE DURATIONS: $\tau/W^{1/3}$ VS Z_o FOR TNT

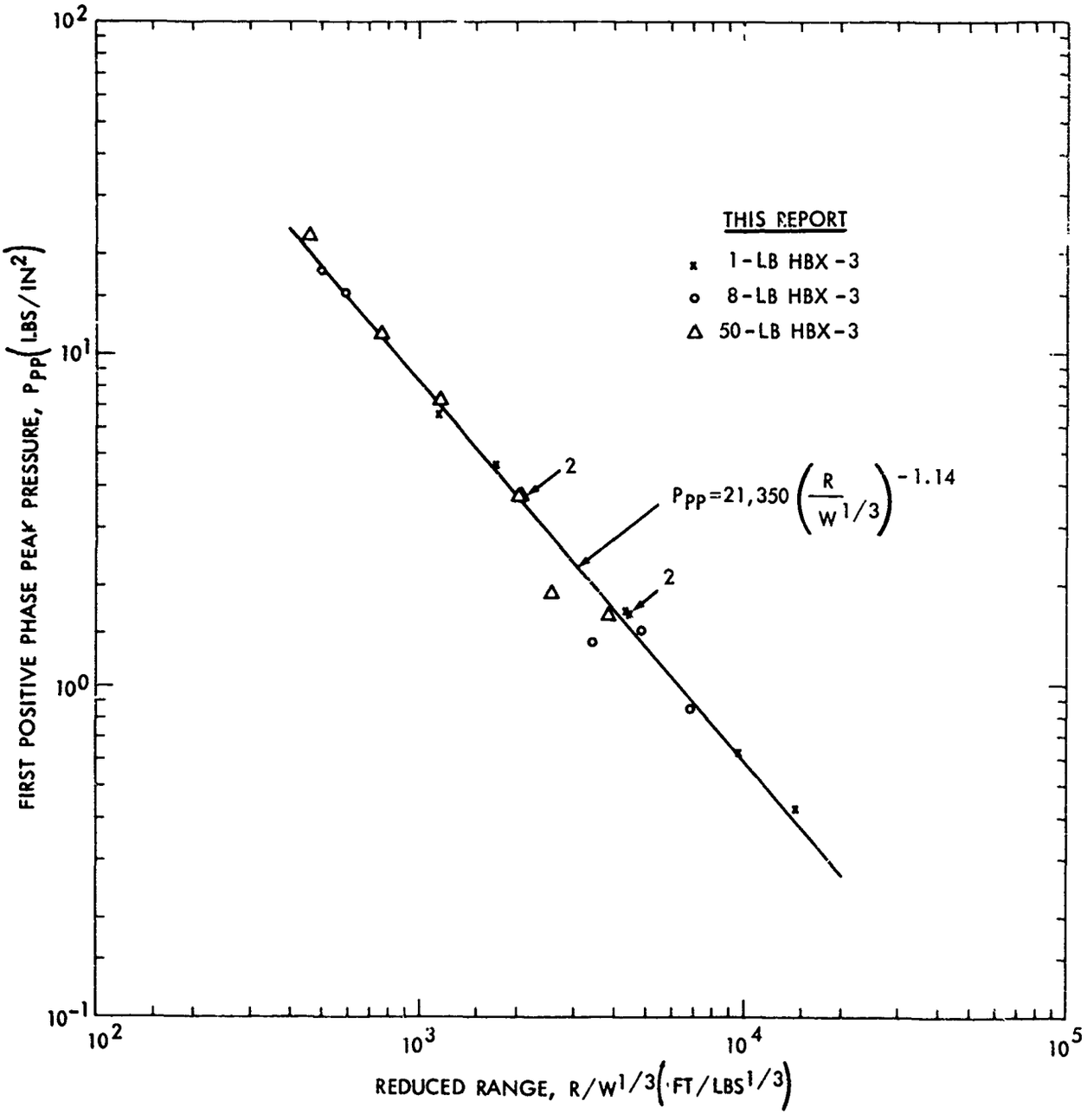

FIG. 11 P_{PP} VS $R/W^{1/3}$ FOR HBX-3

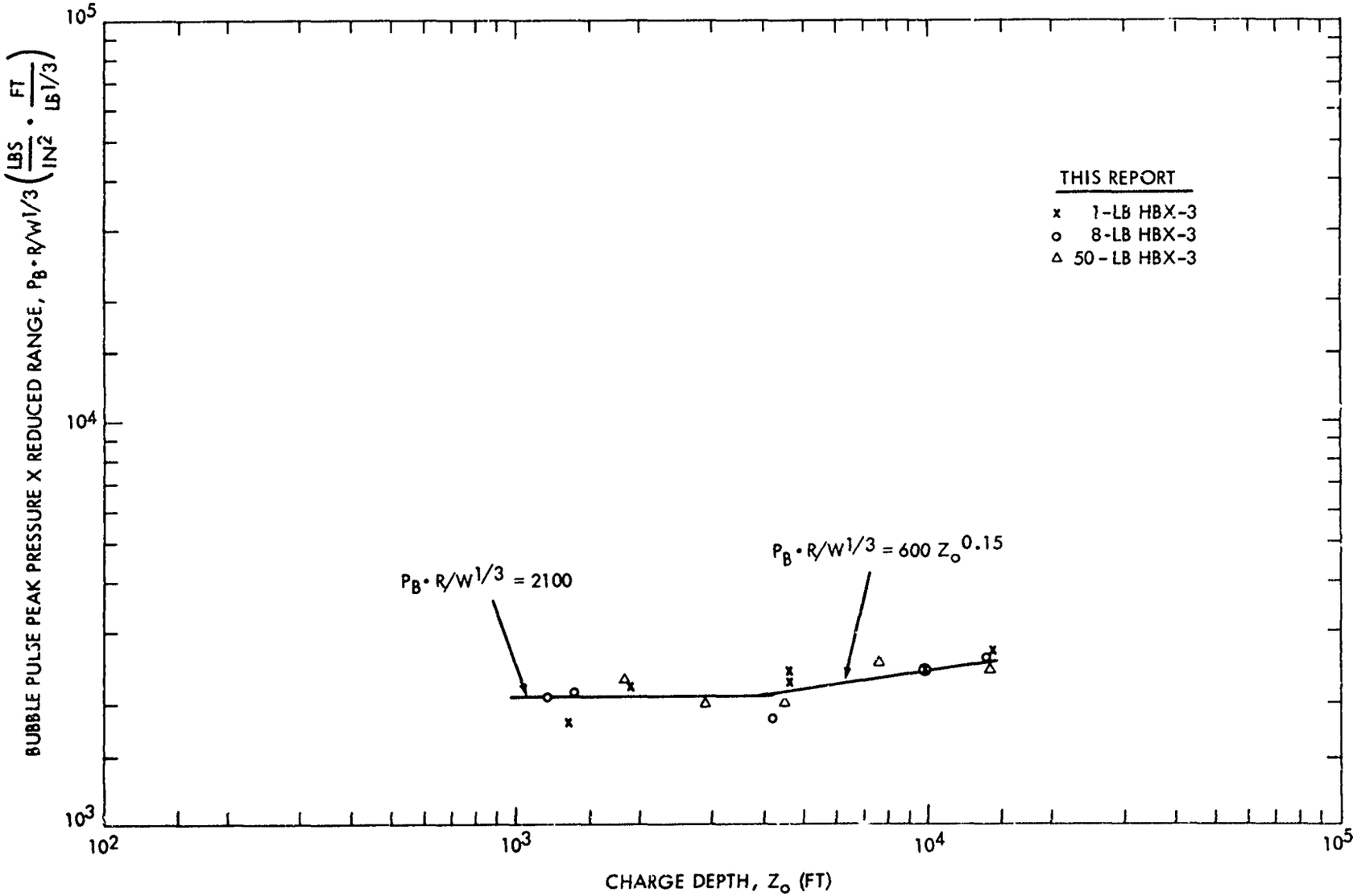

FIG. 12 $P_B \cdot R/W^{1/3}$ VS Z_o FOR HBX-3

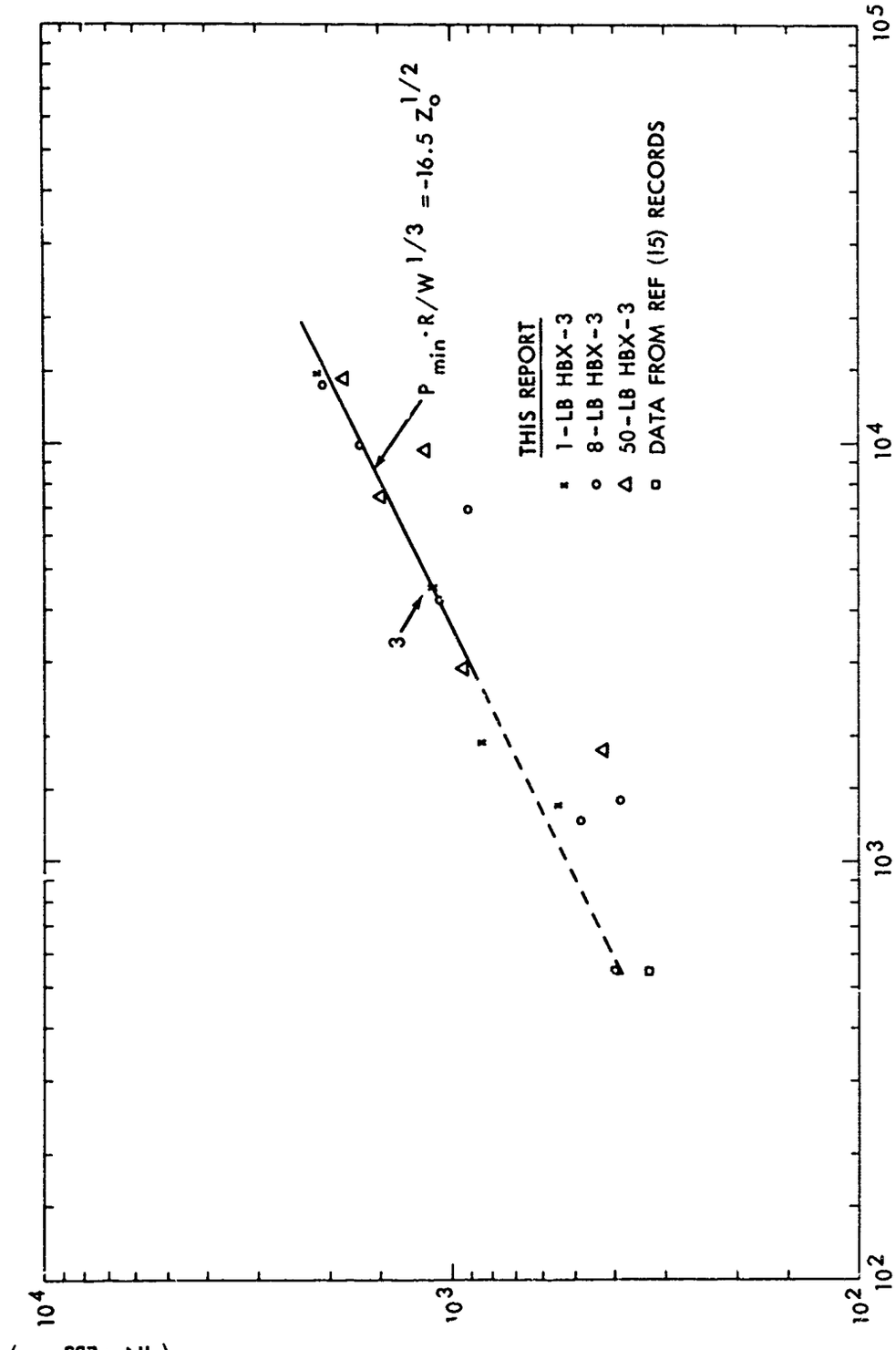

FIG. 13 $P_{min} \cdot R/W^{1/3}$ VS Z_o FOR HBX-3

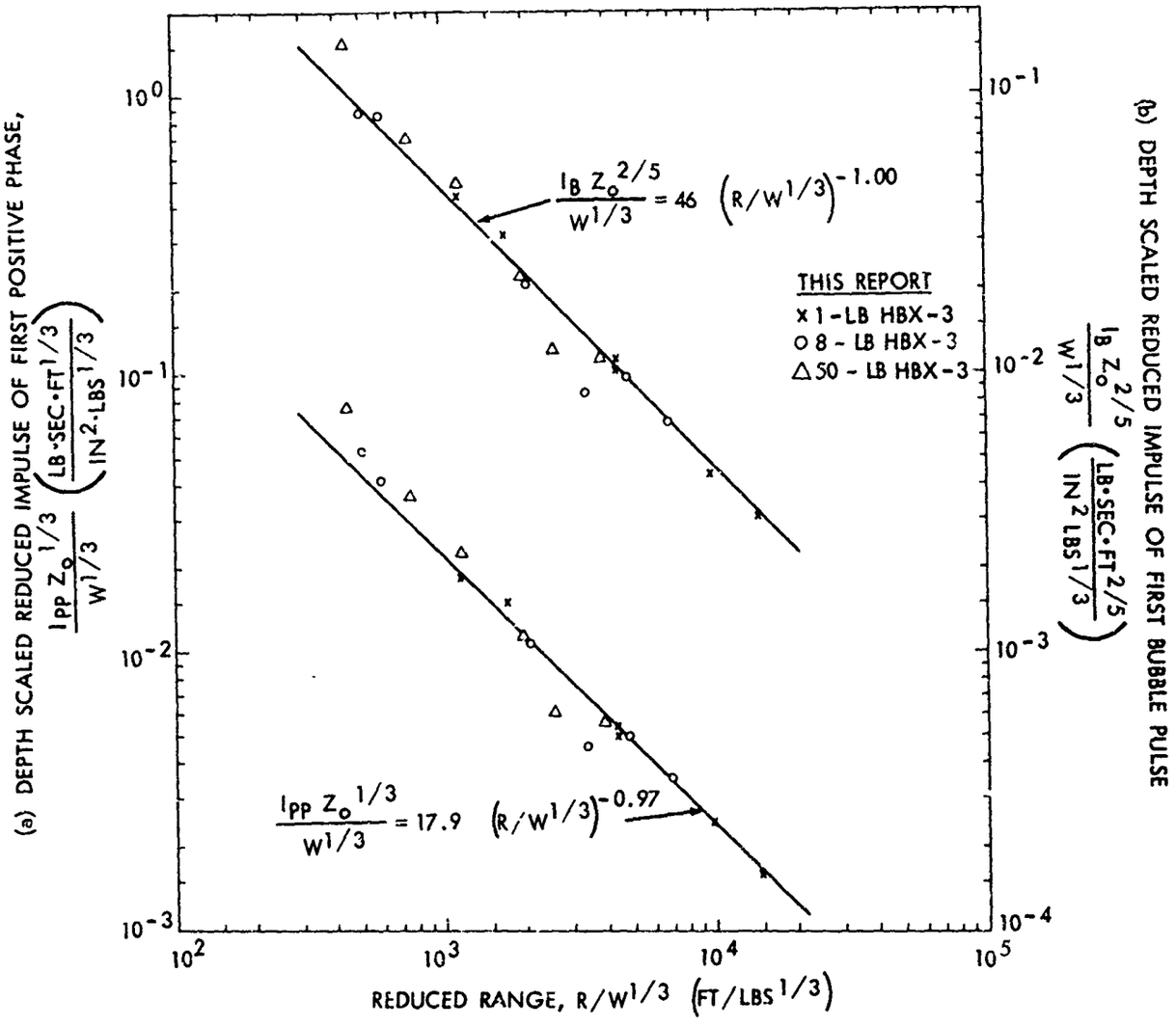

FIG. 14 (a) $I_{PP} Z_o^{1/3}/W^{1/3}$ VS $R/W^{1/3}$ FOR HBX-3

(b) $I_B Z_o^{2/5}/W^{1/3}$ VS $R/W^{1/3}$ FOR HBX-3

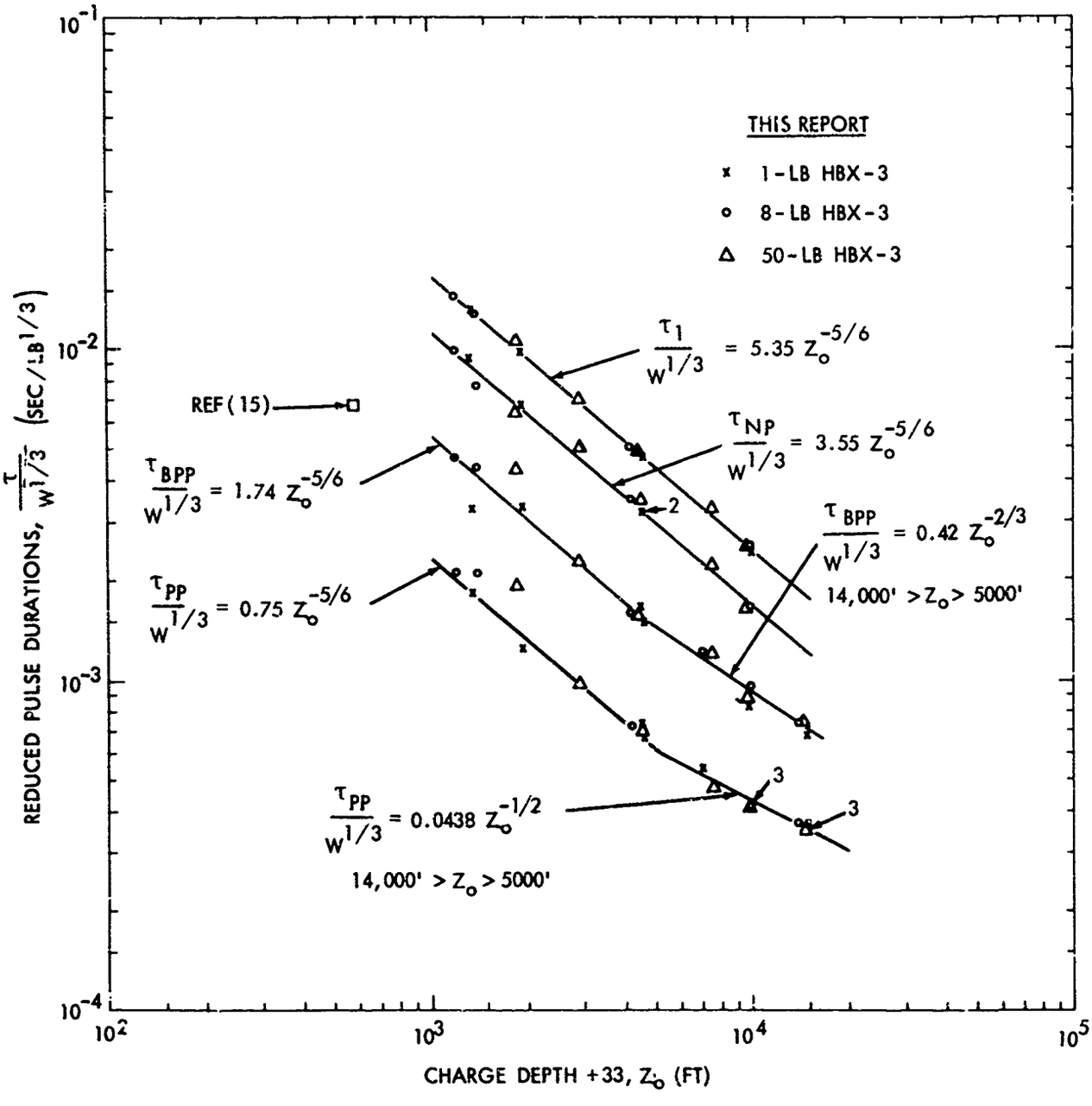

FIG. 15 REDUCED PRESSURE PULSE DURATIONS: $\tau/W^{1/3}$ VS Z_o FOR HBX-3

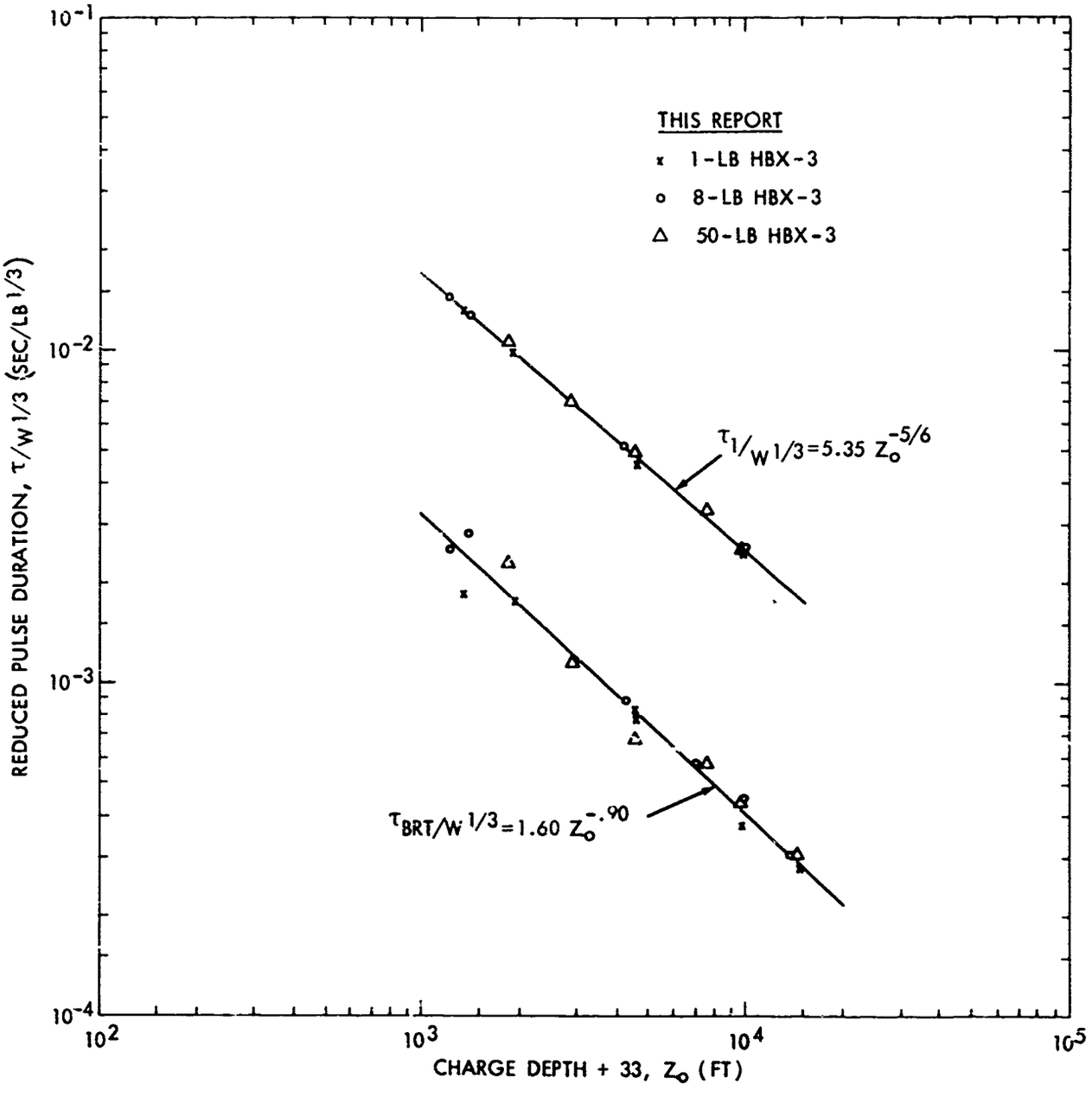

FIG. 16 REDUCED PRESSURE PULSE DURATIONS: $\tau/W^{1/3}$ VS Z_o FOR HBX-3

TABLE II

PRESSURE PULSE MEASUREMENTS

Shot No.	R (FT)	P_{PP} (LBS/IN^2)	$I_{PP} \cdot 10^{-2}$ $\frac{LBS/SEC}{IN^2}$	$E_{PP} \cdot 10^{3}$ $\frac{IN-LB}{IN^2}$	P_B (LB/IN^2)	P_{MIN} (LB/IN^2)	$I_B \cdot 10^{3}$ $\frac{LB-SEC}{IN^2}$	Z_o (FT)	τ_{PP} (MSEC)	τ_{NP} (MSEC)	τ_{BPP} (MSEC)	τ_{BNT} (MSEC)	τ_1 (MSEC)	τ_2 (MSEC)	τ_3 (MSEC)
						TNT (1-lb)									
22	337	25.07	8.71	12.53	9.609	-1.044	14.07	550.3	2.895	15.16	5.64	3.687	21.75	--	--
48	397	19.87	5.688	7.800	6.573	-0.747	7.62	607.8	4.365	13.19	5.495	2.947	20.50	15.04	--
33	426	20.07	6.085	8.930	8.345	-2.481	7.93	640.5	2.355	14.90	4.484	2.537	19.7[illegible]	--	--
49	694	10.68	2.739	2.440	3.90	-0.639	3.48	906.0	1.663	11.15	3.616	1.956	14.[illegible]	10.23	--
67	705	13.04	2.863	3.065	5.168	-0.738	3.63	925.8	2.035	9.640	6.041	2.848	14.[illegible]	10.71	7.982
42	978	7.945	1.801	1.206	3.011	-0.617	1.92	1,191	1.424	8.864	2.923	1.372	11.6[illegible]	8.23	3.96
70	1,059	7.097	1.690	1.634	3.107	-0.499	2.21	1,275	1.477	7.762	3.140	1.900	11.14	--	--
1	1,748	3.89	0.7649	0.289	1.72	-0.430	--	1,961	0.843	5.887	2.126	1.133	7.863	5.762	4.252
27	1,806	4.294	0.858	0.368	1.728	-0.471	1.12	2,036	1.100	5.454	2.048	1.100	7.654	5.479	4.576
45	2,781	2.540	0.424	0.0997	1.073	-0.296	0.499	2,996	0.751	3.969	1.465	0.630	5.410	4.06	3.1[illegible]
10	2,850	2.32	0.434	0.0970	1.12	-0.242	0.519	3,063	0.772	3.710	1.631	0.934	5.416	3.972	3.075
24	4,244	1.551	0.190	0.0679	0.859	-0.283	0.3303	4,444	0.561	2.828	1.122	0.549	3.938	2.867	2.249
52	4,322	1.85	0.252	0.0560	0.874	-0.270	0.289	4,535	0.605	2.841	1.014	0.472	3.91	2.83	2.21
76	7,205	1.000	0.1453	0.01638	0.565	-0.212	0.1662	7,218	0.409	1.938	0.764	0 338	2.684	--	--
77	7,220	0.957	0.133	0.0135	0.571	-0.210	0.154	7,435	0.439	1.793	0.840	0.358	2.59	2.025	1.480
15	13,760	0.413	0.05623	0.0028	0.271	-0.137	--	13,970	0.317	1.043	--	0.173	1.530	1.248	0.934
						TNT (8-lb)									
31	384	56.73	5 .74	140.4	19.08	-2.578	65.8	604.1	11.15	23.80	12.32	6.938	41.89	--	--
26	413	50.9	66.06	160.5	17.9	--	67.4	626	--	--	--	--	40.62	--	--
12	715	24.7	14.03	23.58	8.980	-1.123	18.8	925.3	4.378	20.52	9.888	4.414	29.32	10.26	--
72	951	21.25	8.72	13.71	7.616	-0.990	10.94	1,172	3.438	17.28	6.562	3.562	24.28	17.97	14.50
43	1,059	17.91	8.306	10.47	5.917	-0.934	9.38	1,270	3.538	15.12	7.262	4.136	22.79	16.50	--
69	1,067	18.84	7.282	10.64	6.369	-1.084	9.08	1,284	3.876	15.69	5.750	2.843	22.41	16.84	--
21	1,702	10.96	3.830	63.37	4.188	-0.924	5.02	1,904	2.006	12.05	4.132	2.126	16.18	12.19	10.20
4	1,841	9.311	3.540	2.934	3.67	-0.986	4.504	2,054	1.656	11.92	4.478	2.148	15.72	11.84	9.35
35	1,854	10.60	3.074	2.581	3.251	-0.777	4.068	2,064	1.972	10.70	4.036	2.222	14.89	11.70	9.165
47	2,743	5.796	1.814	1.008	2.484	-0.714	2.228	2,957	1.664	7.926	3.340	1.522	11.11	8.54	--
32	4,130	3.518	1.066	0.383	1.522	-0.674	1.265	4,338	0.980	5.714	2.444	1.222	7.951	5.966	4.822
25	4,199	3.680	1.140	0.4045	1.537	-0.637	1.373	4,405	1.058	6.196	1.800	0.894	8.146	6.064	--
55	4,362	3.564	1.152	0.414	1.497	-0.571	1.397	4,575	0.982	6.132	1.832	0.956	8.069	6.144	--
18	13,119	0.805	0.225	0.0215	0.439	-0.256	0.240	13,330	0.678	3.162	1.018	0.346	3.184	2.550	2.167
36	13,220	0.895	0.245	0.0293	0.636	-0.252	0.2568	13,430	0.602	2.188	1.196	0.364	3.130	2.631	1.991
						TNT (57-lb)									
8	1,660	21.75	15.35	26.96	8.563	-0.492	18.77	1,878	6.337	19.09	14.92	5.129	30.55	22.20	--
29	1,744	21.41	13.74	22.83	7.785	-1.529	16.52	1,956	4.302	20.83	7.549	3.724	26.85	--	--
37	4,104	7.117	4.353	2.965	3.249	-1.186	5.275	4,315	1.925	11.36	3.938	1.937	15.22	17.93	--
20	4,251	7.33	4.048	3.015	3.396	-1.078	4.715	4,446	2.025	11.02	3.746	1.798	14.84	11.56	8.684
3	6,428	4.23	2.072	0.9336	2.059	-0.716	2.280	6,641	1.568	7.085	2.790	1.441	10.10	7.273	4.671
79	6,967	4.61	2.252	1.057	2.48	-0.907	2.501	7,180	1.652	7.235	2.870	1.310	10.20	7.519	5.959
62	14,160	1.951	0.831	0.1775	1.212	-0.548	0.8118	14,370	1.114	3.815	1.771	0.599	5.529	4.281	3.382

TABLE II (continued)

PRESSURE PULSE MEASUREMENTS

Shot No.	R (FT)	P_{FP} (LBS/IN^2)	$I_{FP} \cdot 10^3$ $\frac{LBS/SEC}{IN^2}$	$E_{FP} \cdot 10^3$ $\frac{IN-LB}{IN^2}$	P_B (LB/IN^2)	P_{MIN} (LB/IN^2)	$I_B \cdot 10^3$ $\frac{LB-SEC}{IN^2}$	Z_o (FT)	τ_{FP} (MSEC)	τ_{NP} (MSEC)	τ_{BPT} (MSEC)	τ_{BRT} (MSEC)	τ_1 (MSEC)	τ_2 (MSEC)	τ_3 (MSEC)
						HBX-3 (1-lb)									
46	1,150	6.666	1.674	0.8988	1.577	-0.502	2.437	1,364	1.832	9.225	3.263	1.853	12.91	7.10	6.72
65	1,705	4.65	1.202	0.4727	1.276	-0.501	1.537	1,924	1.232	6.752	3.335	1.760	9.744	6.763	--
51	4,344	1.669	0.3215	0.0653	0.551	-0.258	0.3835	4,557	0.725	3.282	1.657	0.803	4.61	3.69	--
56	4,336	1.638	0.2983	0.0467	0.519	-0.260	0.3472	4,550	0.680	3.25	1.50	0.765	4.70	3.493	2.407
73	9,637	0.625	0.1140	0.00873	0.251	-0.173	0.1095	9,857	0.425	1.669	0.825	0.369	2.463	2.056	1.544
74	14,480	0.428	0.0655	0.00329	0.185	-0.147	0.06582	14,690	0.360	1.180	0.681	0.273	1.813	1.50	1.30
						HBX-3 (8-lb)									
44	1,000	17.77	9.924	13.32	4.107	-0.971	10.18	1,215	4.202	19.59	9.342	4.896	28.70	19.63	14.86
11	1,178	15.19	7.418	8.051	3.540	-0.652	9.316	1,391	4.210	15.60	8.832	5.564	25.38	17.53	--
50	4,022	3.719	1.353	0.4782	0.910	-0.530	1.520	4,235	1.436	6.912	3.162	1.746	10.09	7.818	--
60	6,780	1.36	0.4814	0.06892	0.422	-0.273	0.4998	6,993	1.057	4.536	2.416	1.140	6.732	--	--
71	9,665	1.469	0.4658	0.0794	0.502	-0.348	0.490	9,882	0.828	3.360	1.926	0.904	5.091	4.251	3.743
75	13,705	0.843	0.295	0.0326	0.377	-0.293	0.296	13,920	0.732	2.458	1.468	0.606	3.794	3.394	2.856
						HBX-3 (50-lb)									
63	1,626	22.56	22.83	38.46	5.175	-0.970	27.93	1,846	7.084	23.39	15.93	8.370	38.90	--	--
78	2,760	11.61	9.339	10.90	2.664	-1.249	10.96	2,924	3.537	18.25	8.388	4.288	26.07	20.60	14.24
53	4,259	7.253	5.152	3.669	1.755	-0.981	6.269	4,476	2.579	12.99	5.946	2.483	18.05	15.50	12.52
57	7,326	3.715	2.129	0.7857	1.251	-0.747	2.368	7,531	1.749	8.175	4.421	2.129	12.05	10.21	7.60
59	9,419	1.874	1.057	0.2274	0.625	-0.452	1.165	9,580	1.512	6.174	3.212	1.606	9.295	8.222	6.332
61	14,125	1.635	0.8598	0.1553	0.588	-0.479	0.9159	14,340	1.308	4.384	2.818	1.135	6.823	--	--
						Pentolite (1-lb)									
64	337	28.84	11.14	19.47	13.27	-0.542	15.48	585.1	3.831	14.13	7.379	3.736	21.70	16.14	12.56
68	1,191	7.690	1.669	1.038	3.507	-0.677	2.22	1,410	1.100	8.545	1.916	0.958	10.60	--	--
5	6,441	1.028	0.0576	0.0546	0.606	-0.206	0.218	6,654	0.461	1.992	0.759	0.386	2.839	1.656	1.631
						Nitramex (80-lb)									
38	2,610	12.60	9.655	10.57	3.343	-1.281	11.07	2,825	3.485	17.65	7.191	3.738	24.87	16.99	--
19	2,751	10.09	7.948	7.405	4.055	-0.936	9.736	2,934	3.438	14.31	--	6.785	24.53	--	--
39	6,864	3.563	1.979	0.750	1.138	-0.717	2.038	7,084	2.042	6.496	2.746	2.012	10.55	7.48	5.20
40	10,122	2.115	1.180	0.3151	0.717	-0.505	1.135	10,340	1.318	5.559	2.987	1.374	8.250	6.32	4.46

TABLE III

EMPIRICAL EQUATIONS FOR PRESSURE PULSE CHARACTERISTICS*

Characteristic $Y = k\ Z_o^{\alpha}\ (R/W^{1/3})^{\beta}$
(W in lbs; R and Z_o in ft)

	Y		k	α	β	Limits of Variable
			TNT			
1.	P_{PP}	$\left(\frac{lbs}{in^2}\right)$	20,800	0	-1.13	$14,000 \geq R/W^{1/3} \geq 200$
2a.	P_B	$\left(\frac{lbs}{in^2}\right)$	3,300	0	-1.00	$4,000 \geq Z_o \geq 500$
2b.	P_B	$\left(\frac{lbs}{in^2}\right)$	875	1/6	-1.00	$15,000 \geq Z_o \geq 4,000$
3a.	P_{min}	$\left(\frac{lbs}{in^2}\right)$	-77	1/3	-1.00	$14,000 \geq Z_o \geq 4,500$
3b.	P_{min}	$\left(\frac{lbs}{in^2}\right)$	-4.8	2/3	-1.00	$4,500 \geq Z_o \geq 500$
4.	$I_{PP}/W^{1/3}$	$\left(\frac{lbs \cdot sec}{in^2 \cdot lbs^{1/3}}\right)$	14.7	-1/3	-0.97	$14,000 \geq R/W^{1/3} \geq 500$
5.	$I_B/W^{1/3}$	$\left(\frac{lbs \cdot sec}{in^2 \cdot lbs^{1/3}}\right)$	38.5	-2/5	-1.00	$8,000 \geq R/W^{1/3} \geq 500$
6.	$E_{PP}/W^{1/3}$	$\left(\frac{in \cdot lbs}{in^2 \cdot lbs^{1/3}}\right)$	8,100	-1/5	-2.07	$14,000 \geq R/W^{1/3} \geq 500$
7a.	$\tau_{PP}/W^{1/3}$	$\left(\frac{sec}{lbs^{1/3}}\right)$	0.555	-5/6	0	$4,500 \geq Z_o \quad 500$
7b.	$\tau_{PP}/W^{1/3}$	$\left(\frac{sec}{lbs^{1/3}}\right)$	0.0145	-2/5	0	$22,000 \geq Z_o \geq 4,500$
8.	$\tau_{EP}/W^{1/3}$	$\left(\frac{sec}{lbs^{1/3}}\right)$	3.10	-5/6	0	$14,000 \geq Z_o \geq 500$

* See Fig. 2 and text for definitions of characteristics Y.

TABLE III (continued)

EMPIRICAL EQUATIONS FOR PRESSURE PULSE CHARACTERISTICS

	Y		k	α	β	Limits of Variable
9a.	$\tau_{BPP}/W^{1/3}$	$\left(\frac{sec}{lbs^{1/3}}\right)$	1.10	-5/6	0	$4,500 \geq Z_o \geq 500$
9b.	$\tau_{BPP}/W^{1/3}$	$\left(\frac{sec}{lbs^{1/3}}\right)$	0.155	-3/5	0	$22,000 \geq Z_o \geq 4,500$
10.	$\tau_I/W^{1/3}$	$\left(\frac{sec}{lbs^{1/3}}\right)$	4 34	-5/6	0	$14,000 \geq Z_o \geq 500$
11.	$\tau_{BRT}/W^{1/3}$	$\left(\frac{sec}{lbs^{1/3}}\right)$	1.25	-0.93	0	$14,000 \geq Z_o \geq 500$
			MBX-3			
12.	P_{PP}	$\left(\frac{lbs}{in^2}\right)$	23,500	0	-1.14	$14,000 \geq R/W^{1/3} \geq 400$
13a.	P_B	$\left(\frac{lbs}{in^2}\right)$	2,100	0	-1.00	$4,000 \geq Z_o \geq 500$
13b.	P_B	$\left(\frac{lbs}{in^2}\right)$	600	0.15	-1.00	$15,000 \geq Z_o \geq 4,000$
14.	P_{min}	$\left(\frac{lbs}{in^2}\right)$	-16.5	1/2	-1.00	$14,000 \geq Z_o \geq 3,000$
15.	$I_{PP}/W^{1/3}$	$\left(\frac{lbs \cdot sec}{in^2 \cdot lbs^{1/3}}\right)$	17.9	-1/3	-0.97	$14,000 \geq R/W^{1/3} \geq 500$
16.	$I_B/W^{1/3}$	$\left(\frac{lbs \cdot sec}{in^2 \cdot lbs^{1/3}}\right)$	46.0	-2/5	-1.00	$14,000 \geq R/W^{1/3} \geq 500$
17.	$E_{PP}/W^{1/3}$	$\left(\frac{in \cdot lbs}{in^2 \cdot lbs^{1/3}}\right)$	7,310	-1/5	-2.04	$14,000 \geq R/W^{1/3} \geq 500$
18a.	$\tau_{PP}/W^{1/3}$	$\left(\frac{sec}{lbs^{1/3}}\right)$	0.75	-5/6	0	$5,000 \geq Z_o \geq 1,000$

TABLE XXI (continued)

EMPIRICAL EQUATIONS FOR PRESSURE PULSE CHARACTERISTICS

	Y		k	α	β	Limits of Variable
18b.	$\tau_{PP}/W^{1/3}$	$\left(\frac{\text{sec}}{\text{lbs}^{1/3}}\right)$	0.0438	-1/2	0	$14{,}000 \geq Z_o \geq 5{,}000$
19.	$\tau_{NP}/W^{1/3}$	$\left(\frac{\text{sec}}{\text{lbs}^{1/3}}\right)$	3.55	-5/6	0	$10{,}000 \geq Z_o \geq 1{,}000$
20a.	$\tau_{BPP}/W^{1/3}$	$\left(\frac{\text{sec}}{\text{lbs}^{1/3}}\right)$	1.74	-5/6	0	$5{,}000 \geq Z_o \geq 1{,}000$
20b.	$\tau_{BPP}/W^{1/3}$	$\left(\frac{\text{sec}}{\text{lbs}^{1/3}}\right)$	0.42	-2/3	0	$14{,}000 \geq Z_o \geq 5{,}000$
21.	$\tau_1/W^{1/3}$	$\left(\frac{\text{sec}}{\text{lbs}^{1/3}}\right)$	5.35	-5/6	0	$10{,}000 \geq Z_o \geq 1{,}000$
22.	$\tau_{BKT}/W^{1/3}$	$\left(\frac{\text{sec}}{\text{lbs}^{1/3}}\right)$	1.60	-0.90	0	$14{,}000 \geq Z_o \geq 1{,}000$

APPENDIX A

ENERGY SPECTRA

Energy spectra of the pressure pulses are of interest in determining how the reduced range and depth affect the distribution of the energy with respect to frequency. The energy spectra of the first positive phase and of the total pressure pulse (through one or more bubble periods) have been reported for our data in reference 14, and for the reference 8 data in reference 22. In both cases, however, the depth and range were treated as the same variable.

Reference 14 spectra of the first positive phase show that the maximum values occurred at the lowest frequencies, and this energy value for the 500-ft shots was about 10 dB larger than for the 14,000-ft shots. The spectra for all depths of explosion decreased with increasing depth, converged at a reduced frequency of about 1500 Hz-lb$^{1/3}$ and diverged again as the frequency increased further. At the highest frequency ($\sim$ 20 kHz-lb$^{1/3}$), the energy of the shallowest shots was again about 10 dB larger than that for the 14,000-ft shots. A similar effect was observed in reference 14 for the spectra of the total pressure pulse, except that the maximum (peak) in the spectrum for each depth occurred at the respective bubble frequency of the first bubble oscillation.

The reference 14 and 22 energy spectra and, Weston's energy spectra (reference 23) of shallow water data, were reduced by the square of the impulse; i.e., by $W^{4/3}/R^2$, determined from shallow water explosions. In view of the reduced range and depth dependence upon the impulse determined in this report, all energy spectra* should be reduced by the factor $W^{4/3}/R^2.Z_o^{2/3}$. Such a reduction results in a coincidence of all maximum (peak) energy levels at the low frequency end and also in a coincidence of all spectra at the high frequency end (about 20 kHz-lb$^{1/3}$) of the spectrum, for both types of pulses. Also, the spectra for the first positive phase diverge at the mid-frequencies so that the spectrum for the 14,000-ft explosion depth was larger by 8 to 10 dB than that for the 500-ft shot. Such a divergence reflects a continuous change in the wave form of the first positive phase; i.e., from an exponential to a triangular pulse as the depth increases (see Figure 2). The maximum deviation for the case of the total pulse occurs at the frequency of the first bubble oscillation. Figures A-1 and A-2 are reproductions of Figures 7 and 11 in reference 14 with adjustments in energy level for the effect of depth. The non-conformance of the 500-ft depth spectra at the highest frequency is probably the result of gauge relaxation.

---

* For the shock wave impulse, the range exponent of -0.97 is considered to be -1.00, as Weston assumed. Although the bubble impulse is proportional to $Z_o^{-2/5}$, the energy spectra of the total pulse is more nearly proportional to $(Z_o^{-1/3})^2$ since the energy in the first positive phase predominates over most of the frequency range (references 21 and 22).

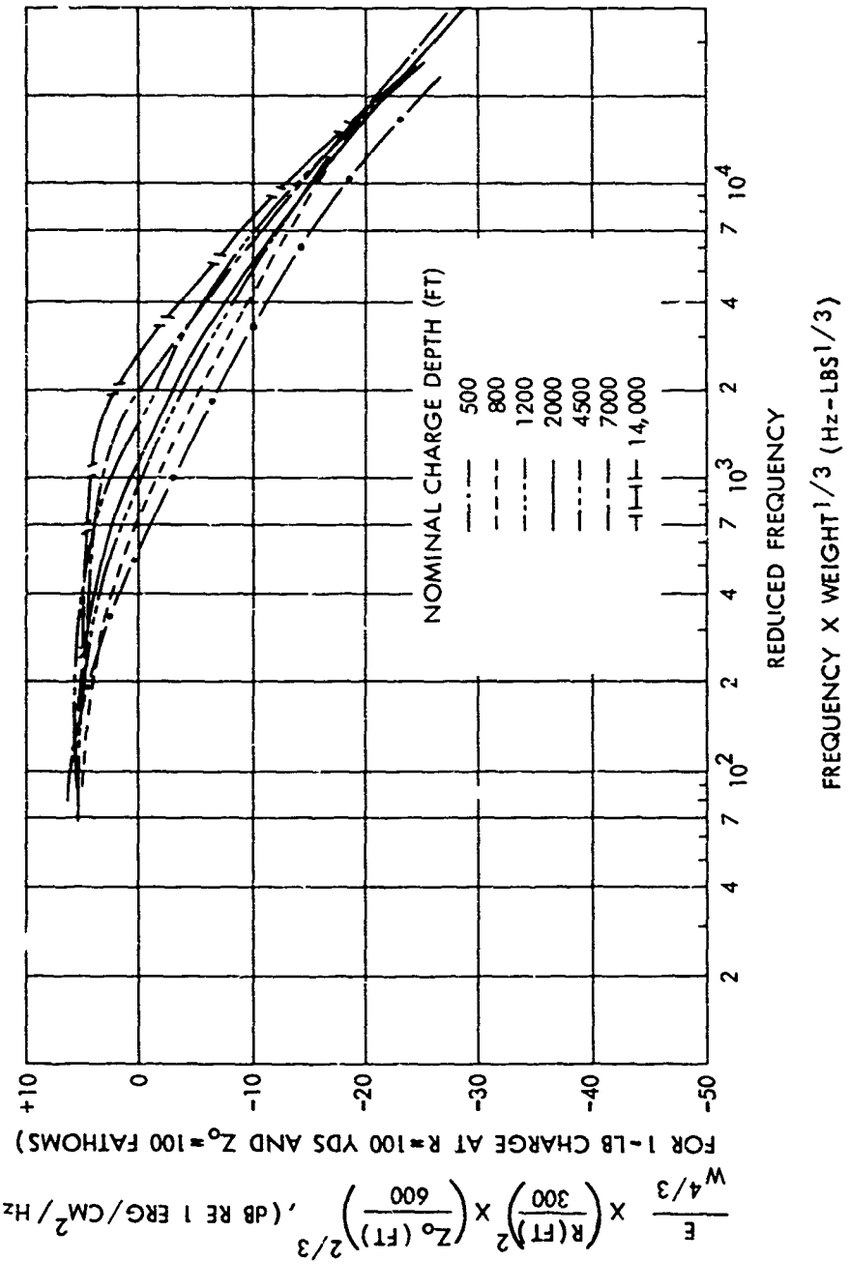

FIG A-1 SHOCK WAVE OCTAVE BAND ENERGY FOR TNT CHARGES

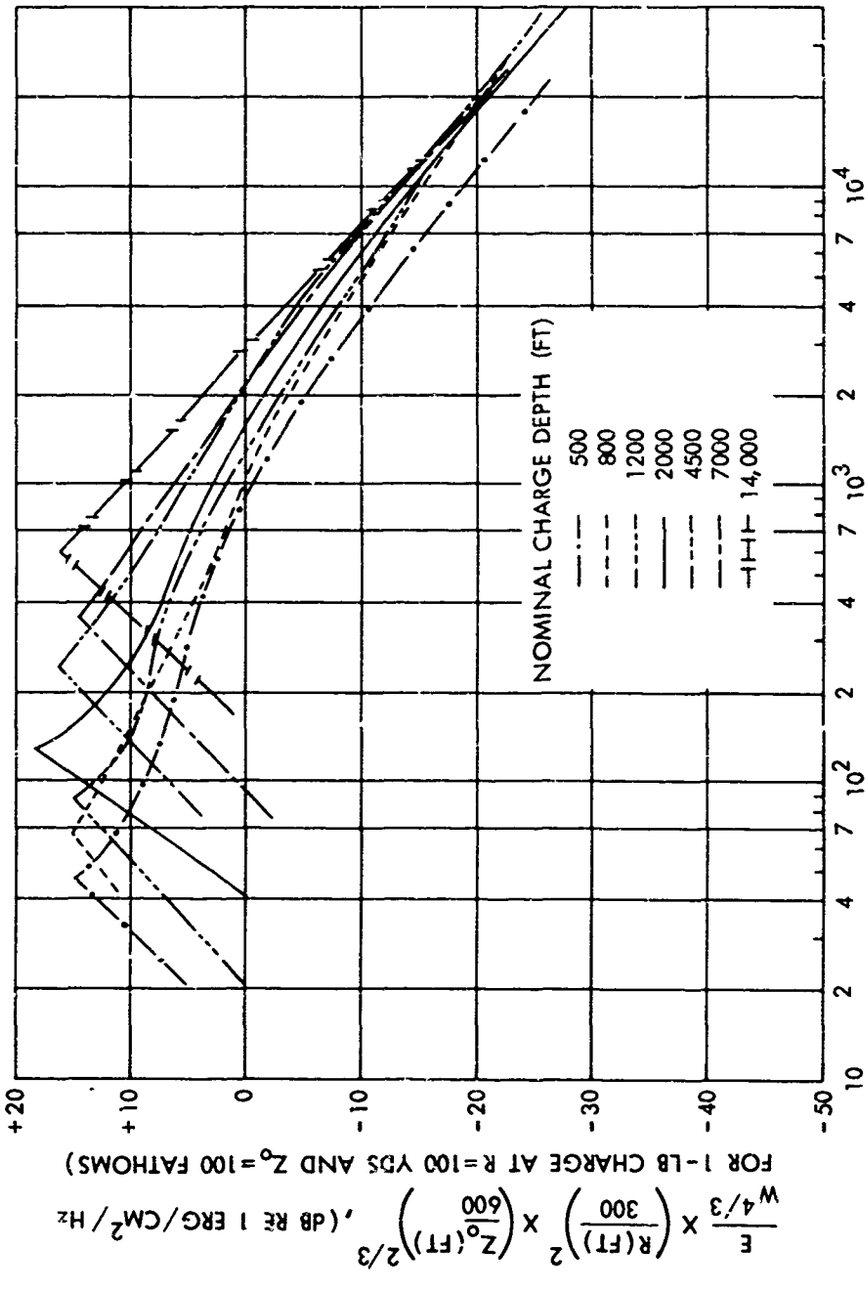

FIG. A-2 TOTAL PULSE OCTAVE BAND ENERGY FOR TNT CHARGES

Unclassified
Security Classification

DOCUMENT CONTROL DATA - R&D

(Security classification of title body of abstract and indexing annotation must be entered when the overall report is classified)

1 ORIGINATING ACTIVITY *(Corporate author)*

U. S. Naval Ordnance Laboratory
White Oak, Silver Spring, Maryland 20910

2a REPORT SECURITY CLASSIFICATION

Unclassified

2b GROUP

3 REPORT TITLE

Pressure-Pulse Characteristics of Deep Explosions as Functions of Depth and Range

4 DESCRIPTIVE NOTES *(Type of report and inclusive dates)*

5 AUTHOR(S) *(Last name, first name, initial)*

John P. Slifko

6 REPORT DATE	7a TOTAL NO OF PAGES	7b NO OF REFS
21 September 1967	iv + 36	23

8a CONTRACT OR GRANT NO

b PROJECT NO ARPA Order 610, Amendment No. 1, NOL Task No. NOL-785/ARPA

c

d

9a ORIGINATOR'S REPORT NUMBER(S)

NOLTR 67-87

9b OTHER REPORT NO(S) *(Any other numbers that may be assigned this report)*

10 AVAILABILITY/LIMITATION NOTICES

Distribution of this report is unlimited.

11 SUPPLEMENTARY NOTES

12. SPONSORING MILITARY ACTIVITY

Advanced Research Projects Agency

13 ABSTRACT

Thirty-eight TNT and 18 HBX-3 charges weighing one, eight, and fifty pounds were fired at depths between 500 and 14,000 ft; pressure-time data were measured directly above at 185-ft depth. The shock wave peak pressure was independent of depth and decayed with reduced range as in the shallow water case. Durations were a function of depth alone. Empirical equations were derived which show that all other pressure-pulse characteristics can be expressed as functions of depth as well as range.

DD FORM 1 JAN 64 1473

Unclassified
Security Classification

14 KEY WORDS	LINK A		LINK B		LINK C	
	ROLE	WT	ROLE	WT	ROLE	WT
Explosions, underwater **Pressure pulses** **Pulse propagation** **TNT** **HBX-3**						

INSTRUCTIONS

1. ORIGINATING ACTIVITY. Enter the name and address of the contractor, subcontractor, grantee, Department of Defense activity or other organization *(corporate author)* issuing the report.

2a REPORT SECURITY CLASSIFICATION. Enter the overall security classification of the report. Indicate whether "Restricted Data" is included. Marking is to be in accordance with appropriate security regulations.

2b. GROUP: Automatic downgrading is specified in DoD Directive 5200.10 and Armed Forces Industrial Manual. Enter the group number. Also, when applicable, show that optional markings have been used for Group 3 and Group 4 as authorized.

3. REPORT TITLE: Enter the complete report title in all capital letters. Titles in all cases should be unclassified. If a meaningful title cannot be selected without classification, show title classification in all capitals in parenthesis immediately following the title.

4. DESCRIPTIVE NOTES: If appropriate, enter the type of report, e.g., interim, progress, summary, annual, or final. Give the inclusive dates when a specific reporting period is covered.

5. AUTHOR(S): Enter the name(s) of author(s) as shown on or in the report. Enter last name, first name, middle initial. If military, show rank and branch of service. The name of the principal author is an absolute minimum requirement.

6. REPORT DATE. Enter the date of the report as day, month, year, or month, year. If more than one date appears on the report, use date of publication.

7a. TOTAL NUMBER OF PAGES. The total page count should follow normal pagination procedure, i.e., enter the number of pages containing information.

7b. NUMBER OF REFERENCES. Enter the total number of references cited in the report.

8a. CONTRACT OR GRANT NUMBER. If appropriate, enter the applicable number of the contract or grant under which the report was written.

8b, 8c, & 8d. PROJECT NUMBER. Enter the appropriate military department identification, such as project number, subproject number, system numbers, task number, etc.

9a. ORIGINATOR'S REPORT NUMBER(S): Enter the official report number by which the document will be identified and controlled by the originating activity. This number must be unique to this report.

9b. OTHER REPORT NUMBER(S): If the report has been assigned any other report numbers *(either by the originator or by the sponsor)*, also enter this number(s).

10. AVAILABILITY/LIMITATION NOTICES. Enter any limitations on further dissemination of the report, other than those imposed by security classification, using standard statements such as:

(1) "Qualified requesters may obtain copies of this report from DDC."

(2) "Foreign announcement and dissemination of this report by DDC is not authorized."

(3) "U. S. Government agencies may obtain copies of this report directly from DDC. Other qualified DDC users shall request through _____."

(4) "U. S. military agencies may obtain copies of this report directly from DDC. Other qualified users shall request through _____."

(5) "All distribution of this report is controlled. Qualified DDC users shall request through _____."

If the report has been furnished to the Office of Technical Services, Department of Commerce, for sale to the public, indicate this fact and enter the price, if known.

11. SUPPLEMENTARY NOTES: Use for additional explanatory notes.

12. SPONSORING MILITARY ACTIVITY. Enter the name of the departmental project office or laboratory sponsoring *(paying for)* the research and development. Include address.

13 ABSTRACT. Enter an abstract giving a brief and factual summary of the document indicative of the report, even though it may also appear elsewhere in the body of the technical report. If additional space is required, a continuation sheet shall be attached.

It is highly desirable that the abstract of classified reports be unclassified. Each paragraph of the abstract shall end with an indication of the military security classification of the information in the paragraph, represented as (TS), (S), (C), or (U).

There is no limitation on the length of the abstract. However, the suggested length is from 150 to 225 words.

14 KEY WORDS. Key words are technically meaningful terms or short phrases that characterize a report and may be used as index entries for cataloging the report. Key words must be selected so that no security classification is required. Identifiers, such as equipment model designation, trade name, military project code name, geographic location, may be used as key words but will be followed by an indication of technical context. The assignment of links, roles, and weights is optional.

GPO 931.721

Naval Ordnance Laboratory, White Oak, Md.
(NOL technical report 67-87)
PRESSURE-PULSE CHARACTERISTICS OF DEEP EXPLOSIONS AS FUNCTIONS OF DEPTH AND RANGE, by John P. Slifko. 21 Sept. 1967. v.p. charts, tables. NOL task 785/ARPA.

UNCLASSIFIED

Thirty-eight TNT and 18 HBX-3 charges weighing one, eight, and fifty pounds were fired at depths between 500 and 14,000 ft; pressure-time data were measured directly above at 185-ft depth. The whook wave peak pressure was independent of depth and decayed with reduced range as in the shallow water case. Durations were a function of depth alone. Empirical equations were derived which show that all other pressure-pulse characteristics can be expressed as functions of depth as well as range.

1. Explosives - Shock waves
2. Explosions, Underwater
3. TNT
4. HBX-3
I. Title
II. Slifko, John P.
III. Project

Abstract card is unclassified.

Naval Ordnance Laboratory, White Oak, Md.
(NOL technical report 67-87)
PRESSURE-PULSE CHARACTERISTICS OF DEEP EXPLOSIONS AS FUNCTIONS OF DEPTH AND RANGE, by John P. Slifko. 21 Sept. 1967. v.p. charts, tables. NOL task 785/ARPA.

UNCLASSIFIED

Thirty-eight TNT and 18 HBX-3 charges weighing one, eight, and fifty pounds were fired at depths between 500 and 14,000 ft; pressure-time data were measured directly above at 185-ft depth. The whook wave peak pressure was independent of depth and decayed with reduced range as in the shallow water case. Durations were a function of depth alone. Empirical equations were derived which show that all other pressure-pulse characteristics can be expressed as functions of depth as well as range.

1. Explosives - Shock waves
2. Explosions, Underwater
3. TNT
4. HBX-3
I. Title
II. Slifko, John P.
III. Project

Abstract card is unclassified.

Naval Ordnance Laboratory, White Oak, Md.
(NOL technical report 67-87)
PRESSURE-PULSE CHARACTERISTICS OF DEEP EXPLOSIONS AS FUNCTIONS OF DEPTH AND RANGE, by John P. Slifko. 21 Sept. 1967. v.p. charts, tables. NOL task 785/ARPA.

UNCLASSIFIED

Thirty-eight TNT and 18 HBX-3 charges weighing one, eight, and fifty pounds were fired at depths between 500 and 14,000 ft; pressure-time data were measured directly above at 185-ft depth. The whook wave peak pressure was independent of depth and decayed with reduced range as in the shallow water case. Durations were a function of depth alone. Empirical equations were derived which show that all other pressure-pulse characteristics can be expressed as functions of depth as well as range.

1. Explosives - Shock waves
2. Explosions, Underwater
3. TNT
4. HBX-3
I. Title
II. Slifko, John P.
III. Project

Abstract card is unclassified.

Naval Ordnance Laboratory, White Oak, Md.
(NOL technical report 67-87)
PRESSURE-PULSE CHARACTERISTICS OF DEEP EXPLOSIONS AS FUNCTIONS OF DEPTH AND RANGE, by John P. Slifko. 21 Sept. 1967. v.p. charts, tables. NOL task 785/ARPA.

UNCLASSIFIED

Thirty-eight TNT and 18 HBX-3 charges weighing one, eight, and fifty pounds were fired at depths between 500 and 14,000 ft; pressure-time data were measured directly above at 185-ft depth. The whook wave peak pressure was independent of depth and decayed with reduced range as in the shallow water case. Durations were a function of depth alone. Empirical equations were derived which show that all other pressure-pulse characteristics can be expressed as functions of depth as well as range.

1. Explosives - Shock waves
2. Explosions, Underwater
3. TNT
4. HBX-3
I. Title
II. Slifko, John P.
III. Project

Abstract card is unclassified.